University of Minnesota
ST. ANTHONY FALL LABORATORY
Engineering, Environmental and Geophysical Fluid Dynamics

Project Report No. 480

Simulation and Characterization of Asphalt Pavement Temperatures

by

William Herb, Mihai Marasteanu and Heinz G. Stefan

Prepared for the
Minnesota Department of Transportation (MNDOT)

September 2006

Abstract

This report summarizes the results of an effort to characterize pavement temperature that includes analysis of measured asphalt temperature data from the MnROAD facility and simulations of pavement temperature using a heat transfer model. The measured pavement temperatures are characterized at daily and seasonal time scales, including daily extreme temperatures and temperature gradients, diurnal cycling, and seasonal variations. A one-dimensional finite difference model is used to simulate pavement temperature based on climate parameters such as air temperature, solar radiation, and wind velocity. The temperature simulations provide more detailed information on temperature gradients in the pavement and on the surface heat transfer components than the measurements, and also help to evaluate the quality of the pavement temperature and climate measurements. Overall, the pavement temperature model is able to simulate asphalt temperature to within a 1 to 2°C mean error, but with higher error for winter conditions due to intermittent snow/ice cover and freeze-thaw processes. The pavement temperature simulations are useful to identify the processes and weather conditions that produce the extreme changes in pavement, such as rapid cooling during precipitation events. The pavement temperature model was also able to simulate pavement temperatures at RWIS sites, and therefore could provide a means to check the quality of RWIS climate and pavement temperature data.

Table of Contents

NOTATIONS AND UNITS

C_p: specific heat (J/kg/°C)
K: thermal conductivity (J/m/s/°C)
dT/dz: derivative of temperature with respect to depth
dT/dt: derivative of temperature with respect to time
H_s: surface heat flux (W/m^2)
RMSE: root mean square error (°C)
t: time (seconds)
T: temperature (°C)
T_a: air temperature
T_p: pavement temperature
T_s: surface temperature (°C)
z: depth (m)
α: thermal diffusivity (m^2/s)
ρ: density (kg/m^3)

1. INTRODUCTION

Weather (climate), along with traffic loading, is a primary factor in determining the service life of pavement. Weather subjects pavement to a variety of effects, including solar radiation, air temperature, moisture, freeze-thaw cycles etc. The focus of this study is on pavement temperatures, and the emphasis is on pavement temperature dynamics, i.e. characterization of pavement temperature over time and depth. Data as well as simulations (modeling results) will be used to achieve the goal.

The mechanical properties of asphalt change substantially with temperature. Surface heat transfer produces high stress gradients near the pavement surface, diurnal temperature cycling may induce fatigue cracks, and freeze-thaw cycles may cause cracking. Both measured temperature data and model simulations provide useful characterizations of pavement temperature and of the heat transfer processes that control temperature. This report summarizes the results of an effort to characterize pavement temperature that includes substantial analysis of measured asphalt temperature data from the MnROAD facility and simulations of pavement temperature using a one-dimensional heat transfer model. The measured pavement temperatures are characterized at diurnal and seasonal time scales, including daily extreme temperatures and temperature gradients, diurnal cycling, and seasonal variations. A one-dimensional finite difference model is used to simulate pavement temperature based on climate parameters such as air temperature, solar radiation, and wind velocity. The temperature simulations provide more detailed information on temperature gradients in the pavement and on the surface heat transfer components than the measurements, and also help to evaluate the quality of the pavement temperature and climate measurements.

2. ANALYSIS OF PAVEMENT TEMPERATURE DATA FROM MNROAD (TEST CELL 33, ASPHALT)

2.1 Data preparation

MNROAD Test cell 33 has seven thermocouples recording temperature at 15 minute intervals at depths of 2.5, 7.5, 12.8, 25.2, 38.1, 43.3, and 60.1 cm, with two thermocouples in the 4" thick asphalt layer (Figure 2.1). 15 minute data were obtained for the period March, 2000 to December, 2005. Small gaps in the data set, e.g. 1 hour, where filled using linear interpolation, while longer gaps where left blank. The pavement surface temperature was extrapolated for each time step from the 2.5 and 7.5 cm deep temperature measurements, using Equation 1:

$$(1) \qquad T_s = T_1 + (T_2 - T_1)\left(\frac{z_1}{z_2 - z_1}\right) + \frac{1}{\alpha}\frac{z_1 z_2}{2}\frac{\partial T_1}{\partial dt}$$

where T_1 and T_2 are the temperatures at depth z_1 (2.5 cm) and z_2 (7.5 cm), respectively, α is the thermal diffusivity of the pavement, and t is time. The first two terms on the right-hand-side of Equation 1 represent a linear extrapolation of the surface temperature, while the last term takes into account the unsteady temperature changes.

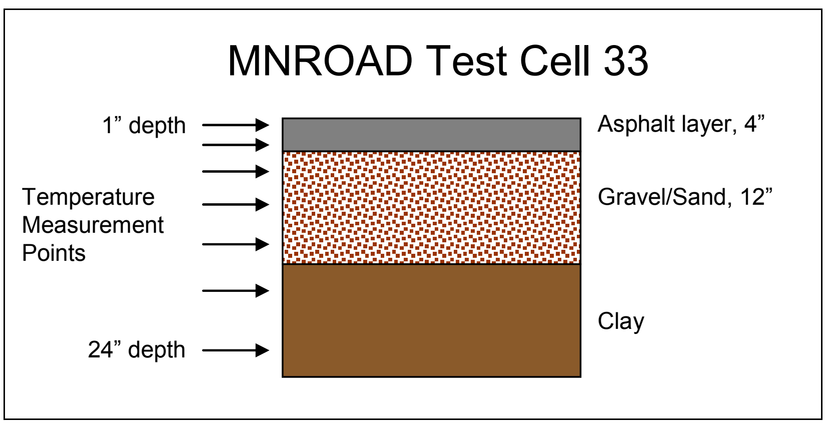

Figure 2.1. Schematic cross section of MnROAD test cell 33, showing the relative position of the seven thermocouples with respect to the pavement, sub-grade, and base layers.

2.2 Pavement temperature parameters related to thermal stress and durability

A number of parameters that characterize pavement temperatures are of interest in the context of pavement durability.

1) The **average pavement temperature** affects both the tensile/compressive stress level and the mechanical material properties.

2) The **temperature gradient over the pavement thickness** produces bending stresses, which are a concern for rigid pavement (concrete) but of less importance for flexible pavement (asphalt). Nonetheless, it should be recognized that temperature and stress gradients may be higher at or near the surface than over the thickness of the pavement.

3) The **diurnal amplitude of pavement temperature** is important for pavement fatigue analysis.

4) The **time rate of change of temperature** is of interest because fast temperature changes give the material less time for plastic creep, and therefore should give higher stress levels.

2.3 Time series of pavement temperature parameters

A basic analysis of pavement temperatures begins with an examination of the seasonal variation over a full year. The seasonal variation of air temperature and solar radiation is given in Figure 2.2, as these two parameters are the primary forcing parameters of pavement temperature. Figure 2.3 gives the seasonal variation of daily surface temperature and average pavement temperature for cell 33, 2004. (In all following discussions, *surface temperature* refers to the extrapolated pavement surface temperature, while *pavement temperature* refers to the depth averaged temperature over the pavement thickness, i.e. 4 inches for Cell 33). The 15 minute data was processed to calculate daily maximum, minimum, and average values of several temperature parameters plotted in Figure 2.3.

The daily mean pavement temperature (Figure 2.3) is substantially higher than the daily mean air temperature (Figure 2.2). Surface and pavement temperature go through very similar seasonal variations, with maximum values in July and minimum values in January. Maximum daily surface temperature reaches 63 °C, which is 11^{o}C higher than the recorded maximum pavement temperature of 52 °C. Diurnal temperature change (daily max – daily min) also exhibits a strong seasonal variation (Figure 2.4), with the highest amplitudes occurring in June. Surface temperature has a significantly higher diurnal change (up to 45 °C) compared to pavement temperature (30 °C).

Monthly temperature summaries are given in Table 2.1, for the period Jan 1, 2001 to Dec 31, 2005.

Figure 2.5 gives the seasonal variation of the extreme (maximum and minimum) values of the temperature gradient (dT/dz) and the rate of change (dT/dt). In general, dT/dz and dT/dt follow the trends of the other temperature parameters, with higher values in the summer and lowest values in the winter. The extreme values of dT/dz and dT/dt are negative; they occur when the pavement surface is cooling during the onset of precipitation in spring, summer and fall. Examples of measured pavement temperatures and climate conditions for an event with a high cooling rate (4/18/2006, 17:00) and a high heating rate (6/8/2004, 11:45) are given in Figure 2.6. The high cooling rate is caused by precipitation after a warm, sunny day, while the high heating rate is caused by an abrupt transition from heavy cloud cover to high solar radiation.

Table 2.1. Monthly pavement and air temperatures for MnROAD test cell 33 (2001 to 2005). Ta = air temperature, Tp = pavement temperature, Ts = surface temperature.

	Jan	Feb	Mar	Apr	May	Jun	Jul	Aug	Sep	Oct	Nov	Dec	All
Mean (C)													
Ta	-7.4	-12.	-3.0	8.5	14.9	19.8	23.3	21.6	14.8	8.3	6.0	-3.6	7.7
Ts	-5.2	-8.1	4.0	14.3	22.5	30.2	35.0	32.9	21.8	11.0	7.0	-2.3	13.4
Tp	-4.9	-7.5	3.6	13.8	22.3	29.6	34.6	32.9	22.3	11.8	7.6	-1.3	13.6
Average Maximum (C)													
Ta	-3.0	-7.0	1.5	13.7	19.9	25.1	28.9	27.5	20.8	13.8	11.1	0.7	12.8
Ts	2.7	0.7	22.1	30.3	40.3	50.7	55.1	53.3	37.8	22.7	16.5	4.3	27.9
Tp	-0.4	-2.3	13.5	22.9	31.8	41.3	46.1	44.8	31.2	18.1	13.0	2.3	21.7
Extreme Maximum (C)													
Ta	6.0	0.3	11.1	27.9	34.9	34.5	34.7	37.5	29.9	29.9	21.7	14.7	37.5
Ts	10.7	19.1	33.6	49.8	59.8	63.7	63.2	64.6	51.9	39.9	27.3	13.0	64.6
Tp	5.2	9.6	23.2	39.0	47.4	52.9	52.8	54.2	42.8	31.4	21.7	9.7	54.2
Mean Diurnal Change (C)													
Ta	7.9	9.6	16.6	16.4	16.9	20.9	20.6	21.0	15.4	11.3	9.2	6.5	14.3
Ts	9.7	11.0	9.3	10.7	10.3	10.7	11.8	12.2	11.3	11.0	10.0	8.7	10.6
Tp	13.2	15.3	28.5	26.5	28.5	33.8	33.7	33.8	25.4	18.8	15.0	11.1	23.6

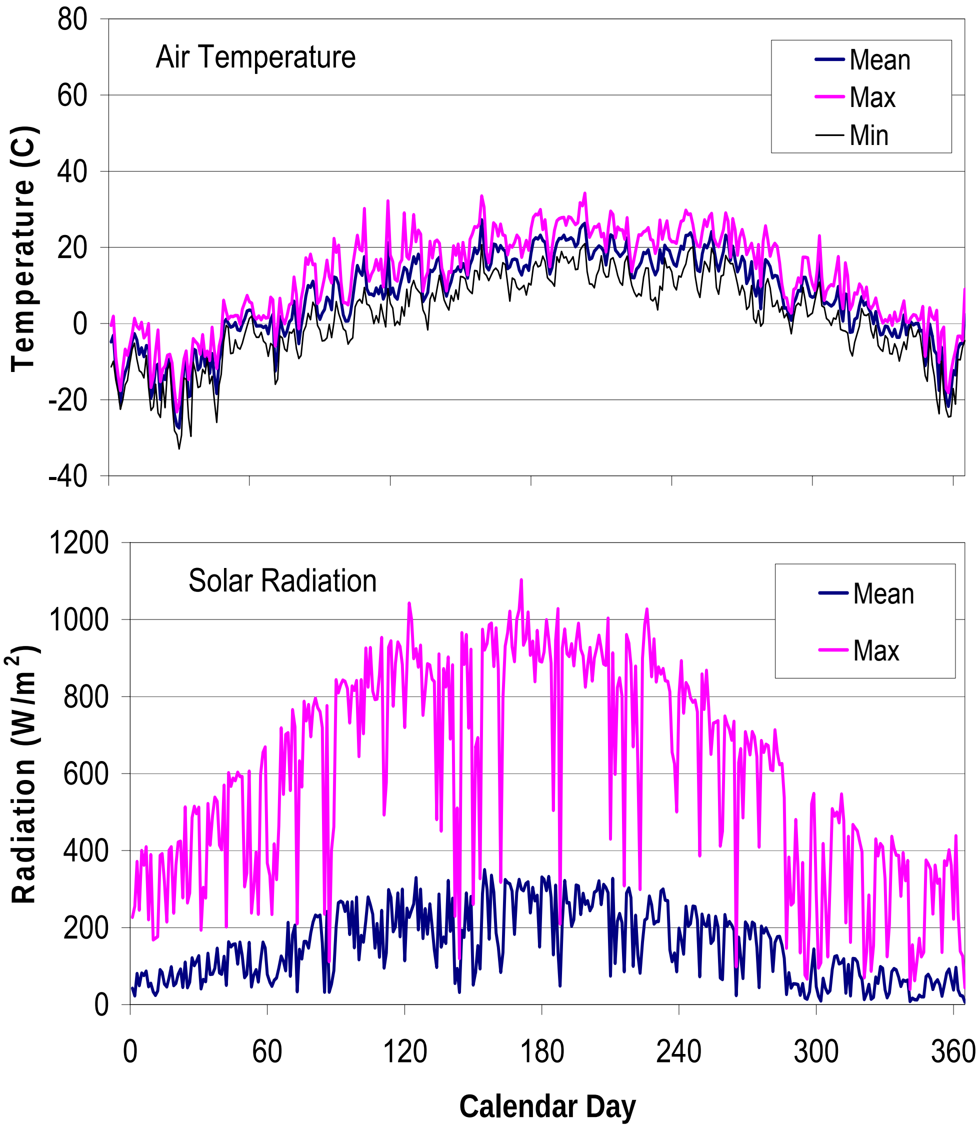

Figure 2.2. Daily mean, maximum, and minimum air temperature and daily mean, and maximum solar radiation, for MnROAD weather station, 2004. Mean solar radiation was calculated over a 24 hour period for each day.

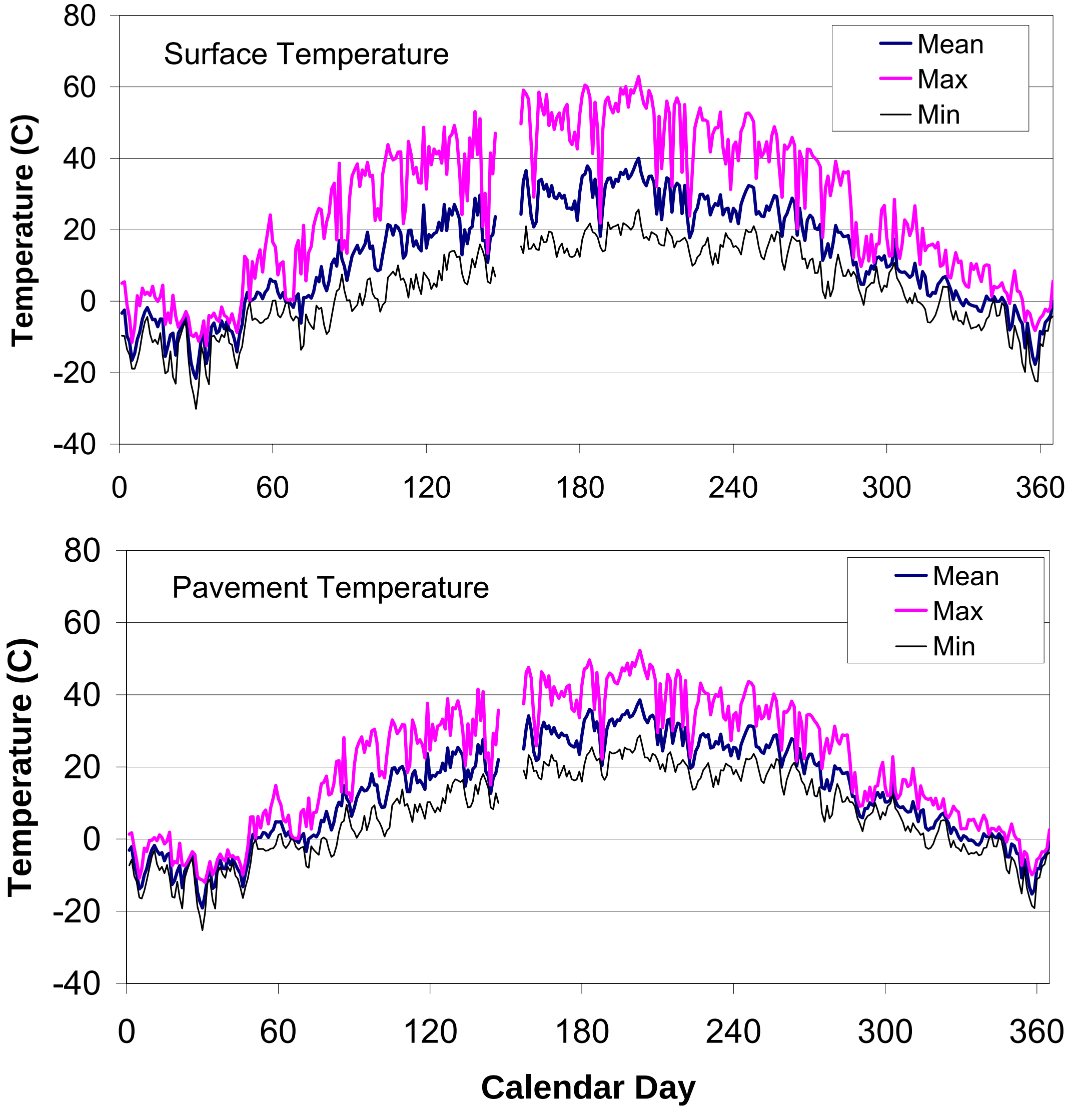

Figure 2.3. Daily mean, maximum, and minimum surface and pavement temperature for Test cell 33, 2004. Pavement temperature is the measured temperature averaged over the pavement thickness.

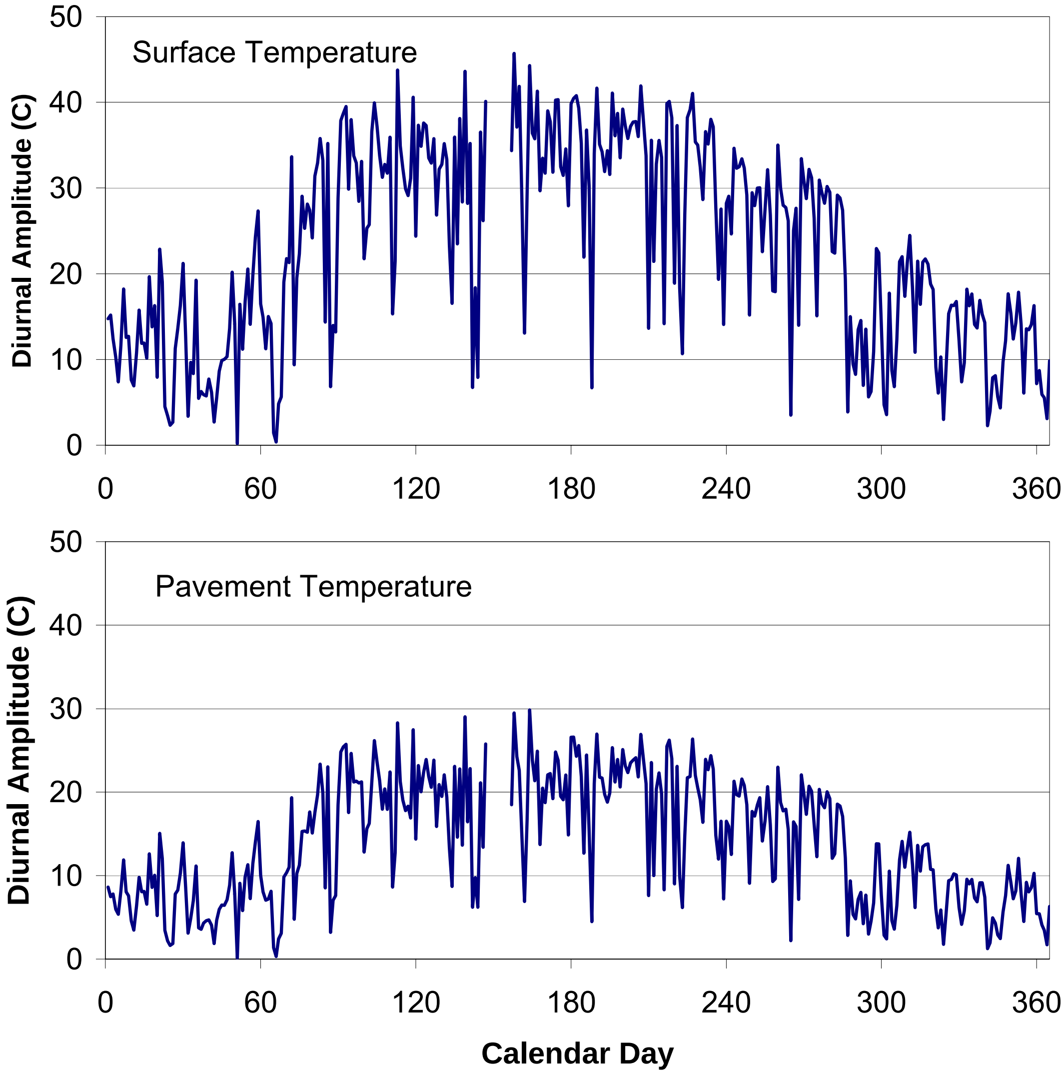

Figure 2.4. Diurnal amplitude of surface and pavement temperature for Test cell 33, 2004.

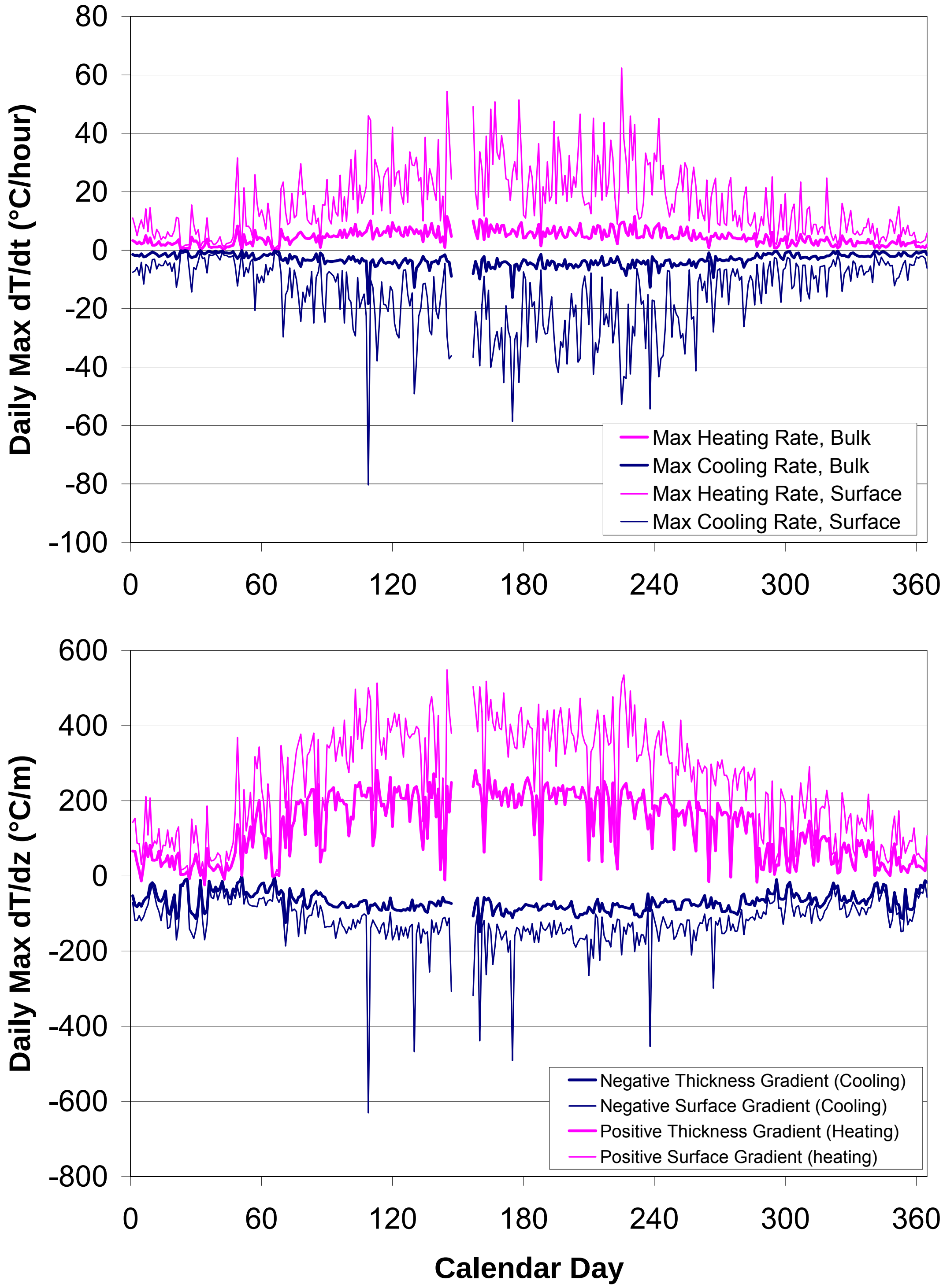

Figure 2.5. Daily extreme temperature gradient (dT/dz) and rate of change of temperature (dT/dt) for Test cell 33, 2004.

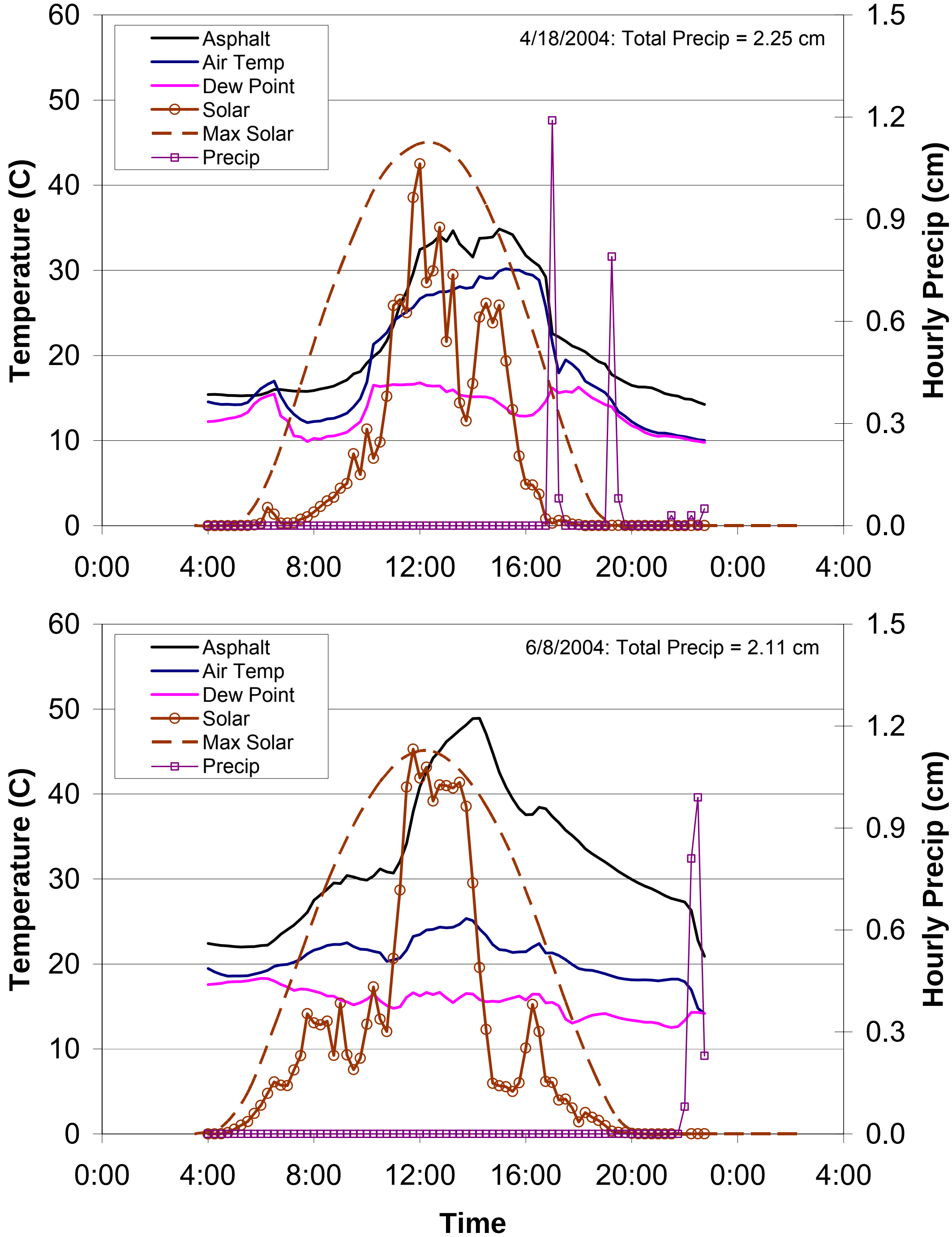

Figure 2.6. Measured pavement temperature and climate conditions for an event giving a high cooling rate (4/18/2006, 17:00) and a high heating rate (6/8/2004, 11:45). “Max Solar” is the clear sky solar radiation, while “Solar” is the measured actual solar radiation.

2.4 Statistical distribution of pavement temperature parameters

Time series illustrate the seasonal variation of temperature parameters and extreme values. To give a statistical characterization of the temperature parameters, histograms were created based on temperature data from test cell 33, for the period Jan 1, 2001 to Dec 31, 2005.

Figure 2.7 gives histograms for daily air temperature, surface temperature, and pavement temperature, recorded at test cell 33; each temperature parameter is placed in 10°C bin. The histograms have several noteworthy features:

1) Maximum daily pavement surface temperature exceeds 60°C on the 12 hottest days of the year and is then 10°C higher than maximum pavement temperature and 30°C higher than maximum daily air temperature. These large differences are attributed to heating by solar radiation.
2) Maximum daily pavement surface and pavement temperatures are far more variable throughout the year than minimum daily values.
3) Minimum daily pavement surface temperatures reach only 30°C on the hottest days of the year, and are less than 5°C warmer than the daily minimum average pavement temperature, and less than 10°C warmer than daily minimum air temperatures.
4) Average daily pavement temperature and average daily surface temperature have very similar distributions; both distributions extend about 10°C higher than average air temperature.
5) The distributions in Figure 2.7 show a double peak to some degree. This is attributed to the distribution of daily solar radiation, given in Figure 2.8.

Figure 2.9 gives the distribution of the diurnal temperature change (daily max – daily min) of the surface, pavement and air temperatures. The asphalt pavement experiences a much greater diurnal temperature change than the air, primarily because of the absorption of solar radiation. Figure 2.10 gives the histogram of the daily extreme temperature gradient (dT/dz) and of the rate of change (dT/dt). While dT/dt is distributed rather symmetrically about zero, dT/dz has a broader distribution of positive values than negative values.

The distributions of the temperature gradient with depth and rate of temperature change are further examined using Equation 2, which gives the basic heat balance on a volume of pavement near the surface (Figure 2.11).

$$(2) \qquad \rho C_p \Delta z \frac{dT_s}{dt} + K\frac{dT}{dz} - H_s = 0$$

The surface heat flux, Hs, enters through the pavement surface, while heat is conducted away at the lower boundary with magnitude K dT/dz. Using Equation 2 and measured pavement temperatures, the surface heat flux, Hs, can be estimated. The distribution of the calculated surface heat flux (Figure 2.12) has a distribution similar to the surface temperature gradient (Figure 2.10). Typical values of these heat budget components for a sunny summer day are plotted in Figure 2.13, where the temperatures and heat budget components are taken from a finite difference simulation, as described in Section 3. Figure 2.13 shows that most of the surface heat transfer is conducted down (K dT/dz), while a smaller fraction produces a change in surface temperature (dT_s/dt).

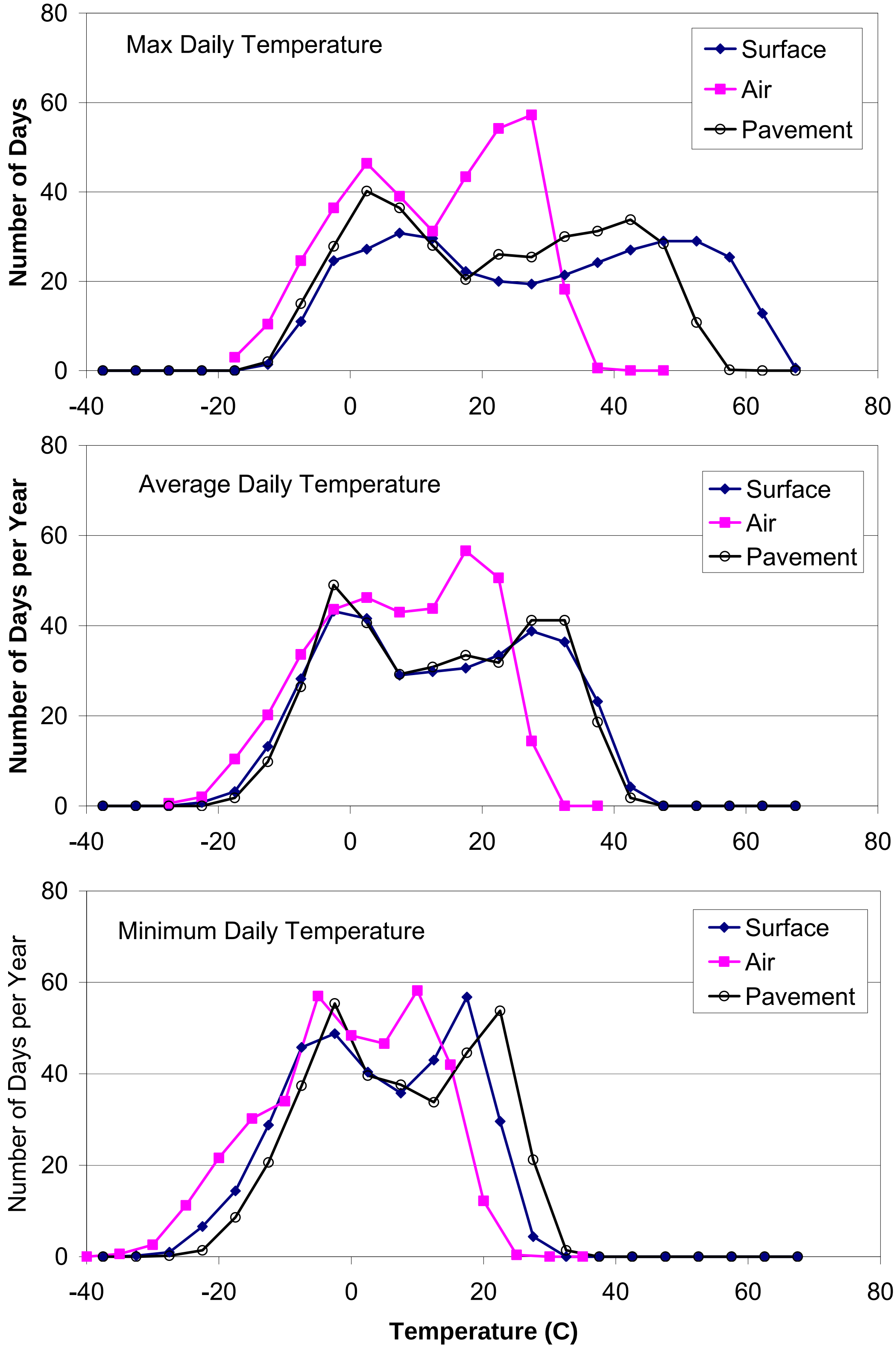

Figure 2.7. Distribution of daily maximum, minimum and average air, surface and pavement temperature for Test cell 33, 2001 – 2005.

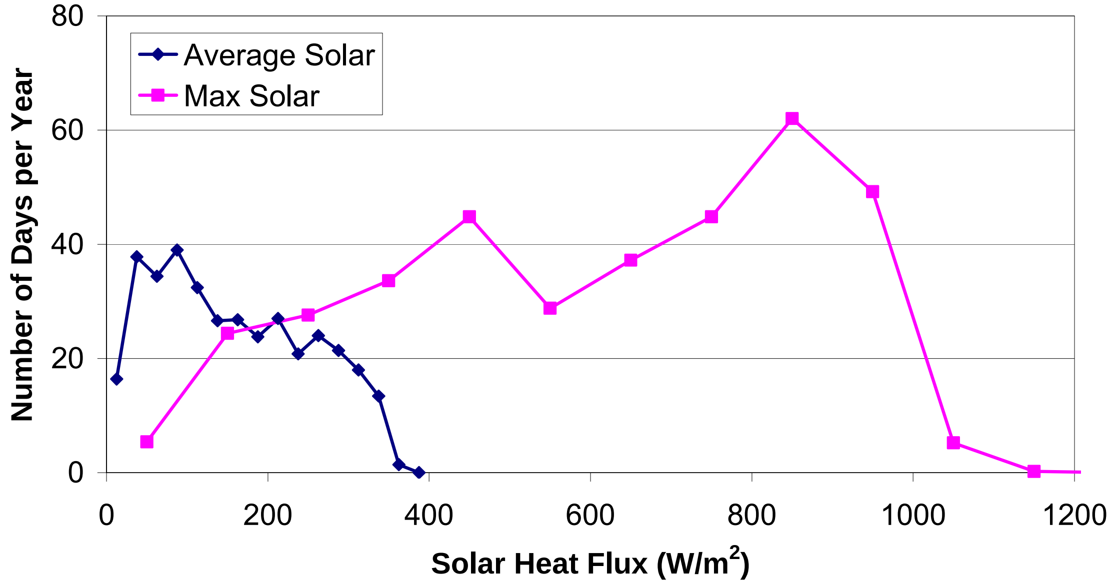

Figure 2.8. Distribution of daily maximum and average solar radiation from the MnROAD weather station, 2001 – 2005. Bill are these daily totals or instantaneous values?

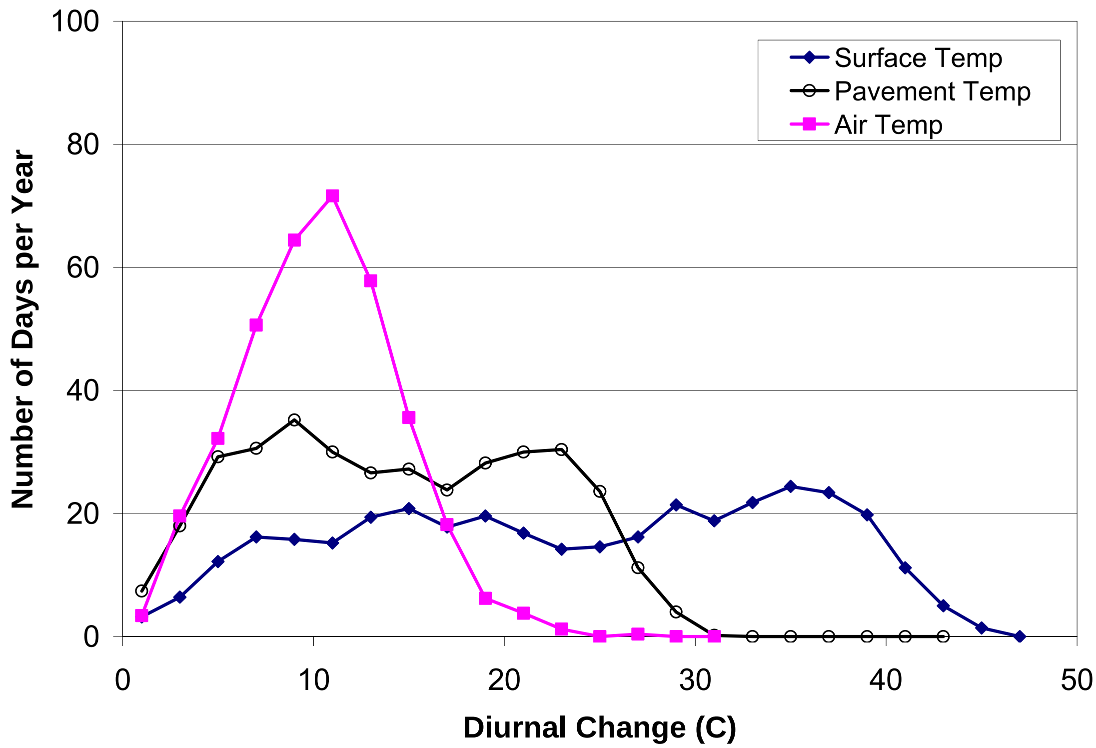

Figure 2.9. Distribution of daily diurnal temperature change (max-min) of the surface and pavement temperature for Test cell 33, 2001 – 2005. Each point represents an average yearly 2.5 °C bin count for the five year period.

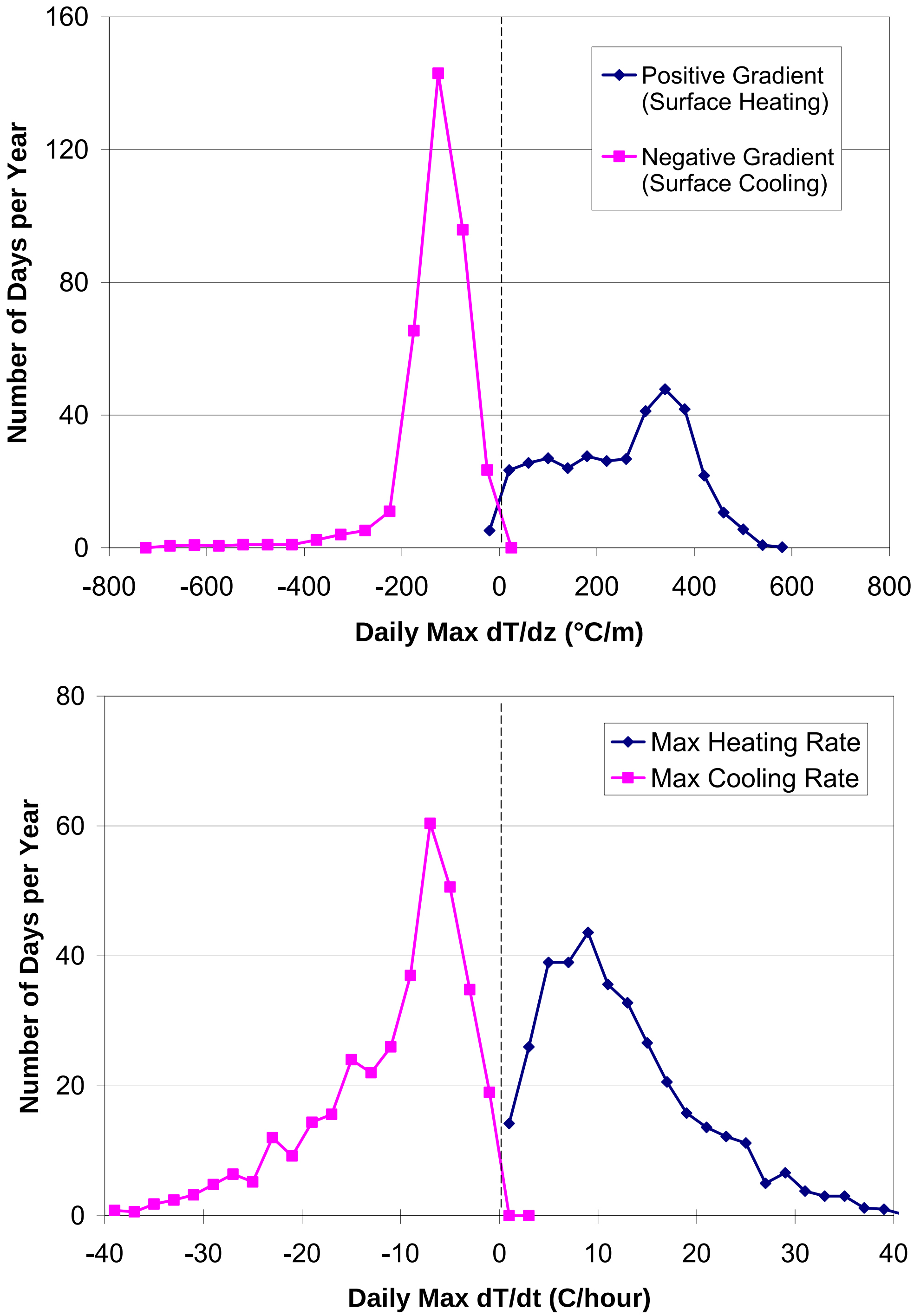

Figure 2.10. Distribution of daily extreme surface temperature gradient (dT/dz) and surface temperature rate of change (dT/dt) for test cell 33, 2001 – 2005. Each point represents an average yearly 2°C bin count for the five year period.

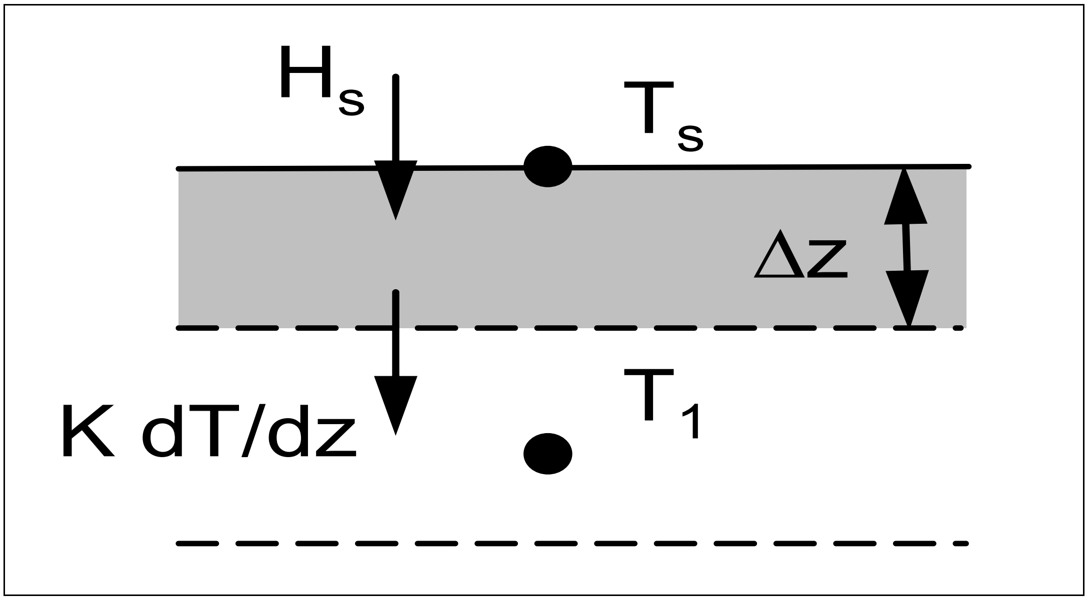

Figure 2.11. Schematic of surface heat transfer components

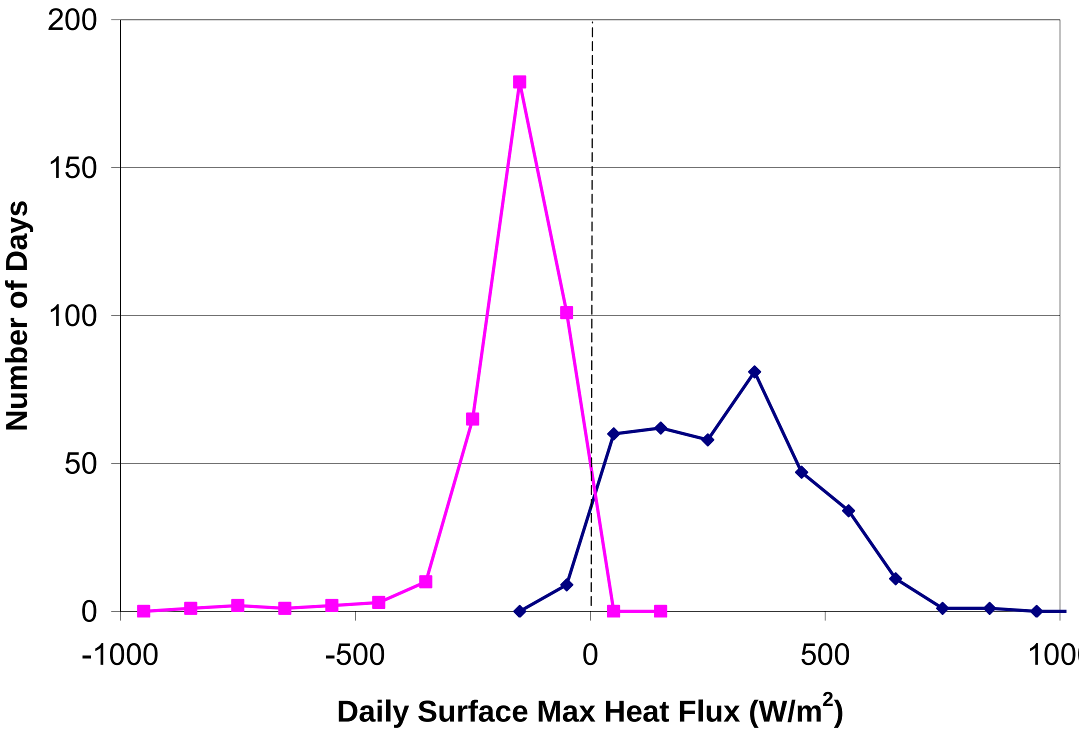

Figure 2.12. Distribution of daily surface heat flux (Hs) for Test cell 33, Jan 1 to Dec 31, 2004.

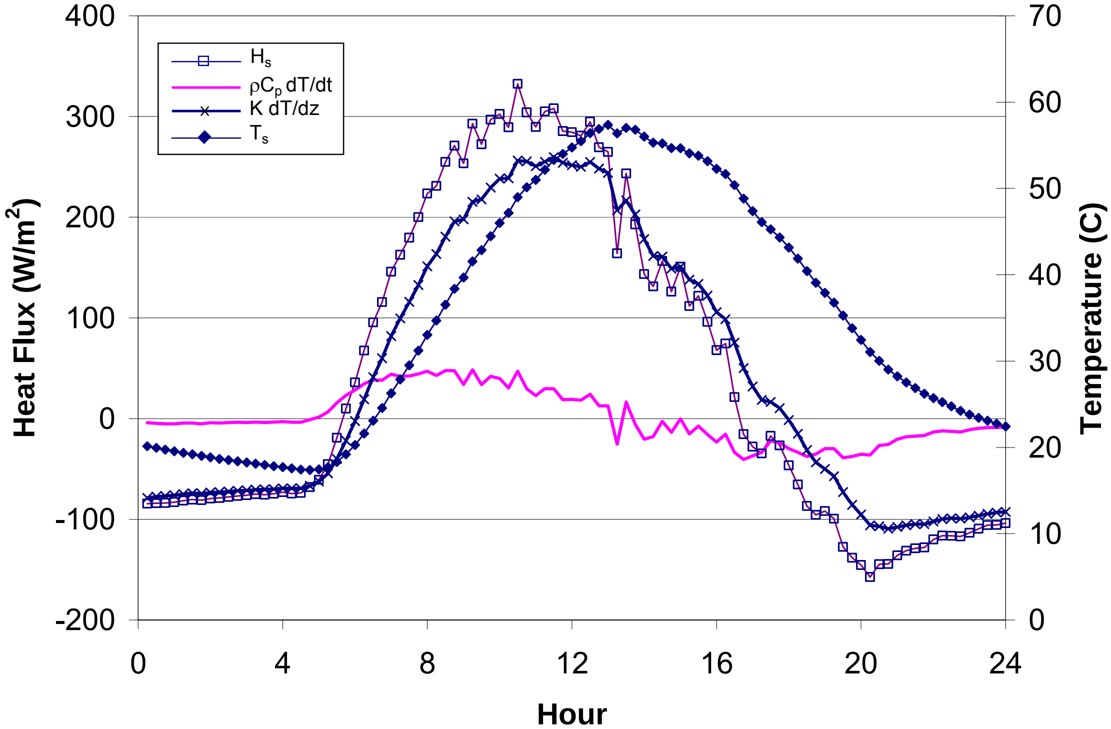

Figure 2.13. Variation of simulated surface temperature (Ts), surface heat flux (Hs), unsteady temperature change ($\rho C_p dT_s/dt$, and vertical heat flux (KdT/dz) over 1 day (June 29, 2004).

2.5 Relationships between pavement temperature parameters

The impact of temperature variation on pavement durability may be dependent on combinations of parameters, rather than the independent variation of single parameters. For example, the combination of low mean temperature and high rate of change of temperature may cause high pavement stress. In this section the interdependency of several important temperature parameters is explored via scatter plots and histograms.

In Figure 2.14 the daily diurnal amplitude of both the surface temperature and the pavement temperature is plotted against daily mean pavement temperature. There is a general trend of increasing diurnal amplitude with increasing mean temperature. Yet the lowest amplitudes occur near the freezing point (0°C) and significant amplitudes exist (20°C) at the lowest mean temperatures (-20 °C). Moderate values of diurnal amplitude occur over a broad range of mean temperatures, e.g. days with 30°C surface temperature diurnal amplitude occur over the range of -10 to 35°C mean temperature.

Spatial and temporal gradients also tend to increase with increasing pavement temperature. The rate of change of temperature for both heating and cooling events increase with increasing surface temperature, with heating and cooling events having similar distributions (Figure 2.15, upper panel). Daily peak values of the vertical temperature gradient (dT/dz) also increase with increasing surface temperature, but positive values correspond to surface heating exceed negative values corresponding to surface cooling.

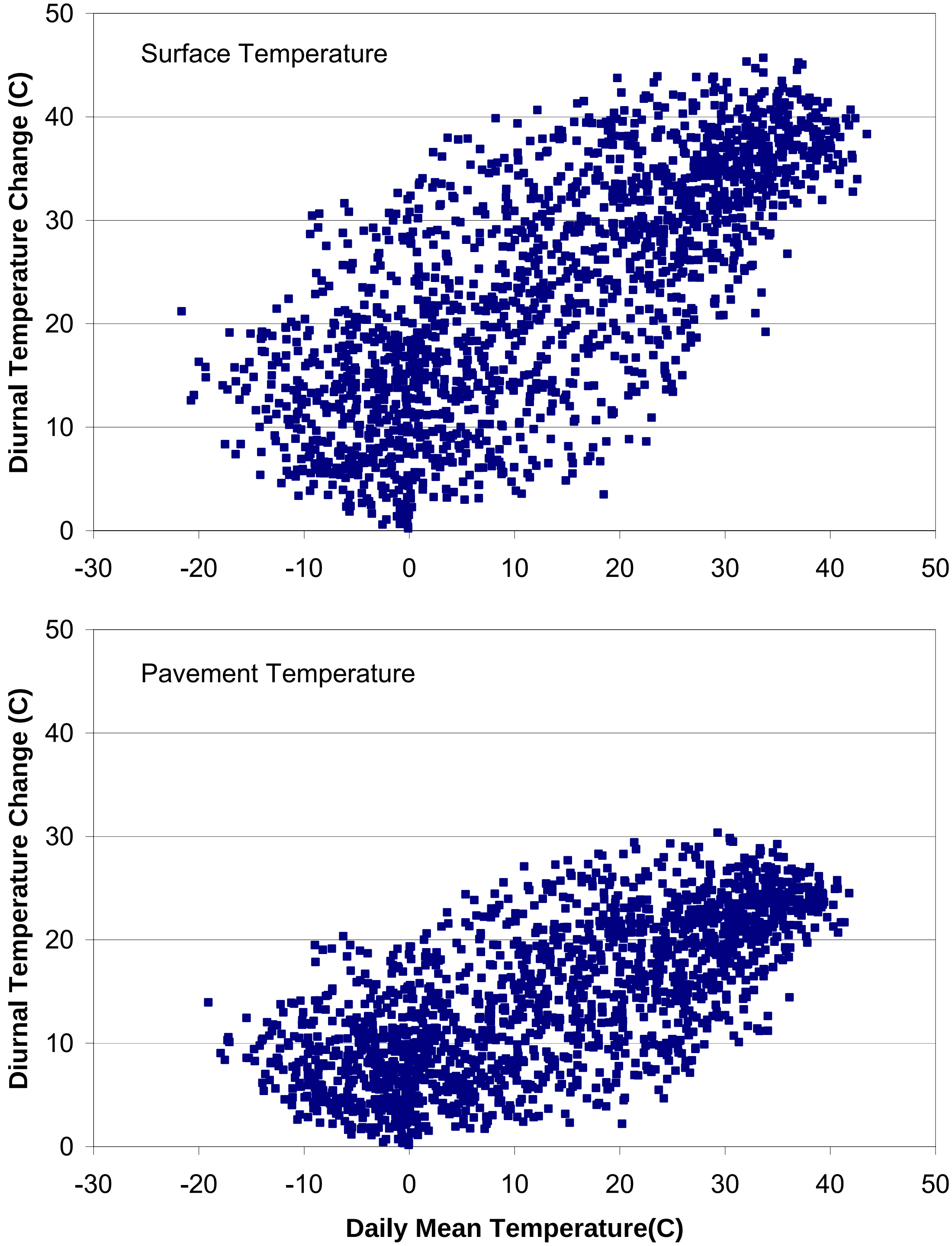

Figure 2.14. Diurnal change (daily max – daily in) versus daily mean temperature for surface temperature and pavement temperature, test cell 33, Jan 1, 2001 – Dec 31, 2005.

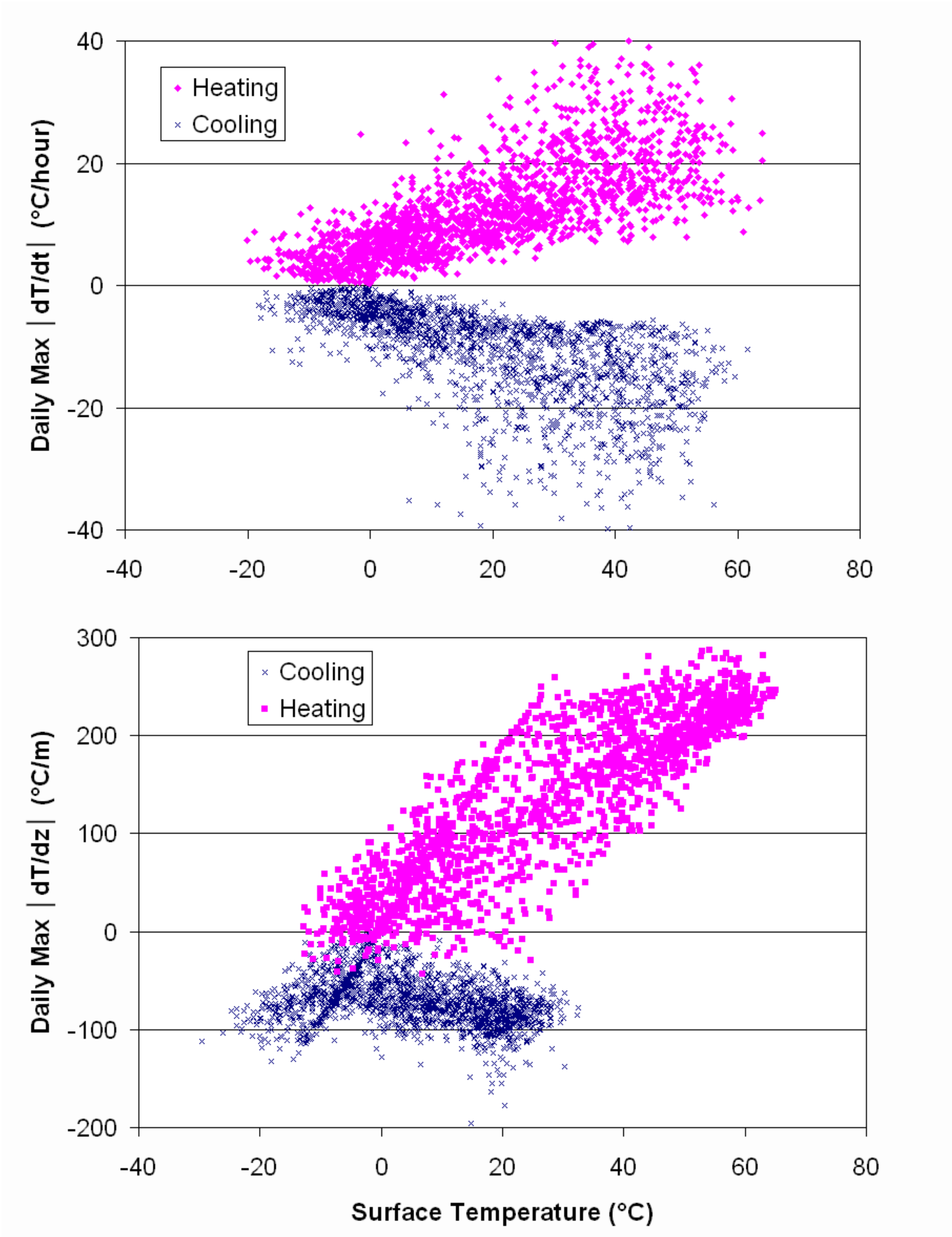

Figure 2.15. Daily extreme temperature gradient (dT/dz) and rate of change (dT/dt) surface temperature for test cell 33, Jan 1, 2001 – Dec 31, 2005.

2.6 Conclusions from pavement temperature data analysis

- Daytime maximum pavement temperature greatly exceeds maximum air temperature, with surface temperatures of up to 63 °C (145 °F) in mid-summer, with corresponding maximum air temperatures of 35 °C (95 °F).
- In general, temperature gradients due to heating are larger than those due to cooling, and surface temperature gradients are higher than the gradient across the thickness of the pavement.
- Surface temperature gradients can be up to 5 °C/cm, and temperature rate of change can be up to 40 °C/hour.
- The highest negative temperature gradients occur during precipitation events, producing tensile surface stress.
- Diurnal amplitude tends to increase with increasing mean temperature, but significant amplitudes exist at cold temperature.
- Daily max, min, and average pavement temperature and diurnal amplitude are not smoothly distributed, but have two peaks that appear to be driven by the distribution of solar radiation.

3. ASPHALT PAVEMENT TEMPERATURE SIMULATION

While the measured pavement temperatures provide a wealth of information on the dynamics of pavement temperature, computer simulations can provide additional information on the underlying mechanisms of temperature dynamics, including information on the components of heat transfer between the pavement and the atmosphere, detailed temperature profiles in the pavement and base layers, and the relationship of material properties to temperature dynamics. The pavement temperature model presented in this section was partially developed at SAFL under a contract with the Minnesota Pollution Control Agency, "Development and Implementation of a Tool to Predict and Assess the Impact of Stormwater Runoff on Trout Streams".

3.1 Model description

Model Summary

The heat transfer model is one dimensional; temperature is modeled vs. depth, assuming horizontal uniformity. Surface heat transfer is modeled using measured weather parameters: air temperature and humidity, solar radiation, precipitation, and wind speed. Conduction of heat into the pavement, sub-grade, and soil is modeled using a finite difference model, with separate material properties for each layer. The model output is temperature vs. depth and time, stored in a text file. The time step of the simulation is largely dependent on the available weather data – a 15 minute time step was used for the simulations discussed in this report. The simulation can be started at any time of year with an initial temperature profile.

Model Inputs

Required inputs to the pavement temperature model include:

1) Climate data: Air temperature (°C), relative humidity (%), wind speed (m/s), and solar radiation (W/m^2). For dry weather periods, it is sufficient to specify climate data at one hour time intervals to simulate surface temperatures. To accurately capture the dynamics of surface temperature prior to storm events, climate data at 10 to 15 minute interval are preferable. Latitude, longitude, and elevation for the site to be simulated are also required for the algorithm to estimate cloud cover.

2) Surface data: Albedo, emissivity, and aerodynamic roughness.

3) Pavement/soil data: Thermal diffusivity and specific heat of the pavement layer; thermal diffusivity of the sub-grade and base layers. Infiltration is assumed to be zero and the soil and pavement moisture properties are not considered.

4) Initial conditions: An initial vertical pavement/soil temperature profile is specified for an arbitrary number of points, which are then interpolated to the node locations of the model.

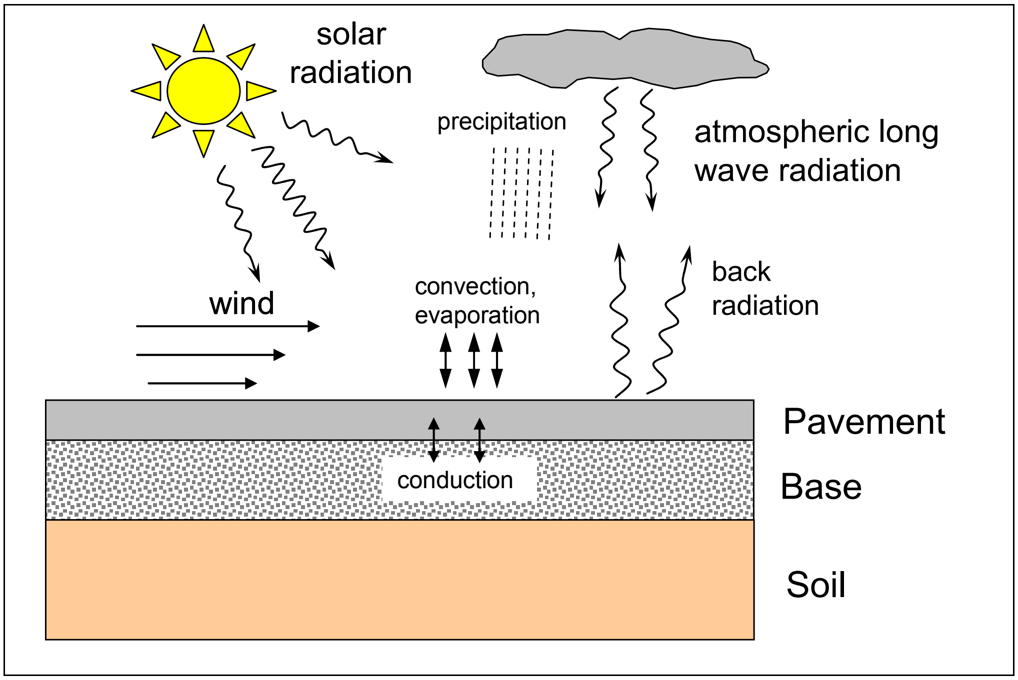

Figure 3.1 Schematic diagram of the processes considered in the pavement temperature model.

3.2 Model formulation

<u>Heat Conduction Model</u>

The heat conduction model uses an implicit finite difference formulation to solve the unsteady heat conduction equation for the vertical pavement/soil profile. The model uses thinner layers for the pavement or the near surface subgrade layers, e.g. 2 cm, and thicker layers towards the lower boundary, e.g. 1 m. As a result, good simulation results are possible with, e.g. 15-20 layers. The model does not presently include moisture dependent thermal properties.

<u>Surface heat transfer formulation</u>

The net vertical heat transfer at the pavement surface includes components due to long wave radiation, short wave (solar) radiation, evaporation, convection, and runoff. The heat transfer formulations used in this study are based on those given by Edinger (1974) for lake and reservoir surfaces, but are applied to pavement and soil by adjusting parameters appropriately. Details of the surface heat transfer formulation are given in Appendix I.

3.3 Model calibration

The surface temperature model was run using 15 minute climate data from the MnROAD facility (Albertville, MN). The model was calibrated and verified using measured pavement temperature data for concrete and asphalt test sections from MnROAD. Seven years of 15 minute climate data was available (1999-2005), six years of asphalt temperature data (Test cell 33) and one year of concrete temperature data (Test cell 38 (2004). Precipitation received in each time step is assumed to completely run off the pavement, so that no standing water is carried over to the next time step, and infiltration is assumed to be zero. The simulations were run using a total soil depth of 10 m, and for the time period April 1 to September 30 for each year of data using either a 15 minute or 60 minute time step.

The following parameter values were obtained by minimizing the root-mean-square error (RMSE) of the simulated and measured pavement temperature values. Values of RMSE will be given later. Surface heat transfer parameters such as albedo and emissivity were calibrated to minimize the simulation error compared to the upper thermocouple node (2.5 cm below the surface). Measured temperatures at other depths were used to calibrate the pavement and soil thermal diffusivity values.

Table 3.1. Calibrated parameter values for asphalt, for the period April 1– September 30, 2004.

Parameter	Value
solar albedo	0.14 (calibrated)
surface heat/moisture transfer coefficient for forced convection	0.0015 (calibrated)
coefficient for natural convection	0.0015
wind sheltering coefficient	1.0
pavement emissivity	0.94
(density · specific heat) pavement	2.0e06 J/m^3/°C
pavement thermal diffusivity	3.0e-07 m^2/s (asphalt) (calibrated) 7.0e-07 m^2/s (concrete) (calibrated)
soil thermal diffusivity	1.0e-06 m^2/s (calibrated)

3.4 Model sensitivity

The sensitivity of the simulated temperatures to several key input parameters are given in Table 3.2. Overall, the emissivity of the pavement had the most influence on surface temperature. An increase in emissivity causes a rather uniform decrease in surface temperature, i.e. both the daytime and nighttime temperatures decrease. The simulated temperatures were relatively insensitive to the sub-soil parameters. The sensitivity to the wind sheltering coefficient is notable, indicating that unquantified wind sheltering from trees, buildings, and surface topography introduces uncertainty into temperature simulations.

Table 3.2. Average surface temperature (°C) increase for a 10% increase in the parameter value listed in the first column. Temperatures for the asphalt test section were simulated from Jan 1 to Dec 31, 2004.

Parameter	Overall Average	Average Daily Max	Average Daily Min	Average Amplitude
pavement emissivity	-0.416	-0.542	-0.374	-0.168
coefficient for natural convection	-0.171	-0.319	-0.102	-0.216
wind sheltering coefficient	-0.169	-0.337	-0.094	-0.243
surface heat/moisture transfer coefficient for forced convection	-0.158	-0.321	-0.083	-0.239
solar albedo	-0.118	-0.286	-0.040	-0.246
pavement (density · specific heat)	0.050	-0.556	0.361	-0.917
pavement thermal diffusivity	0.029	-0.283	0.192	-0.475
soil thermal diffusivity	0.003	0.001	0.025	-0.023

3.5 Comparison of simulated and measured pavement temperatures (snowless season)

Excellent agreement between simulated and measured asphalt and concrete temperature was obtained for all essentially snow-free months (April-September) using either 15 minute or 60 minute time steps. For 2004, the overall RMSE is 1.5°C for asphalt and 1.2°C for concrete. Time series of simulated and measured surface temperature for asphalt and concrete for June/July (Figure 3.2) and August/September (Figure 3.3) illustrate a high level of agreement. Figure 3.4 gives a direct comparison of simulated hourly surface temperatures versus hourly averaged measured temperatures. The slope of the relationship between measured and simulated surface temperature is very close to 1:1 and the intercept is less than 1°C. Tables 3.4, 3.5, and 3.6 summarize the accuracy of the temperature simulations (r^2, RMSE) on a monthly basis and for the entire simulation period. The model was calibrated using 2004 data, but works quite well for the other five years of measured asphalt temperatures (Table 3.6).

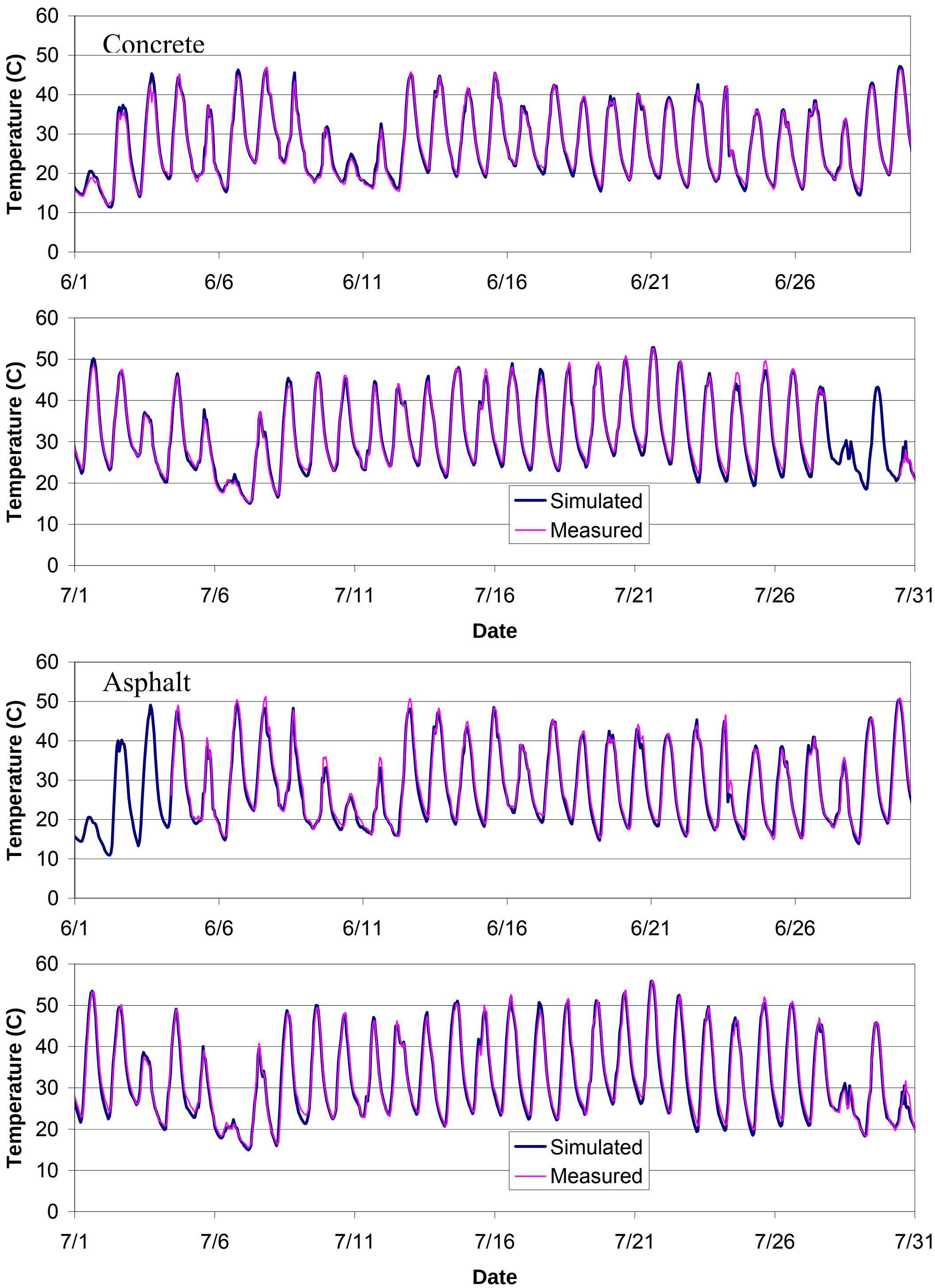

Figure 3.2. Simulated and measured pavement temperature (2.5 cm depth) for June and July, 2004, MnROAD Test cells 33 (asphalt) and 38 (concrete), 1 hour time step.

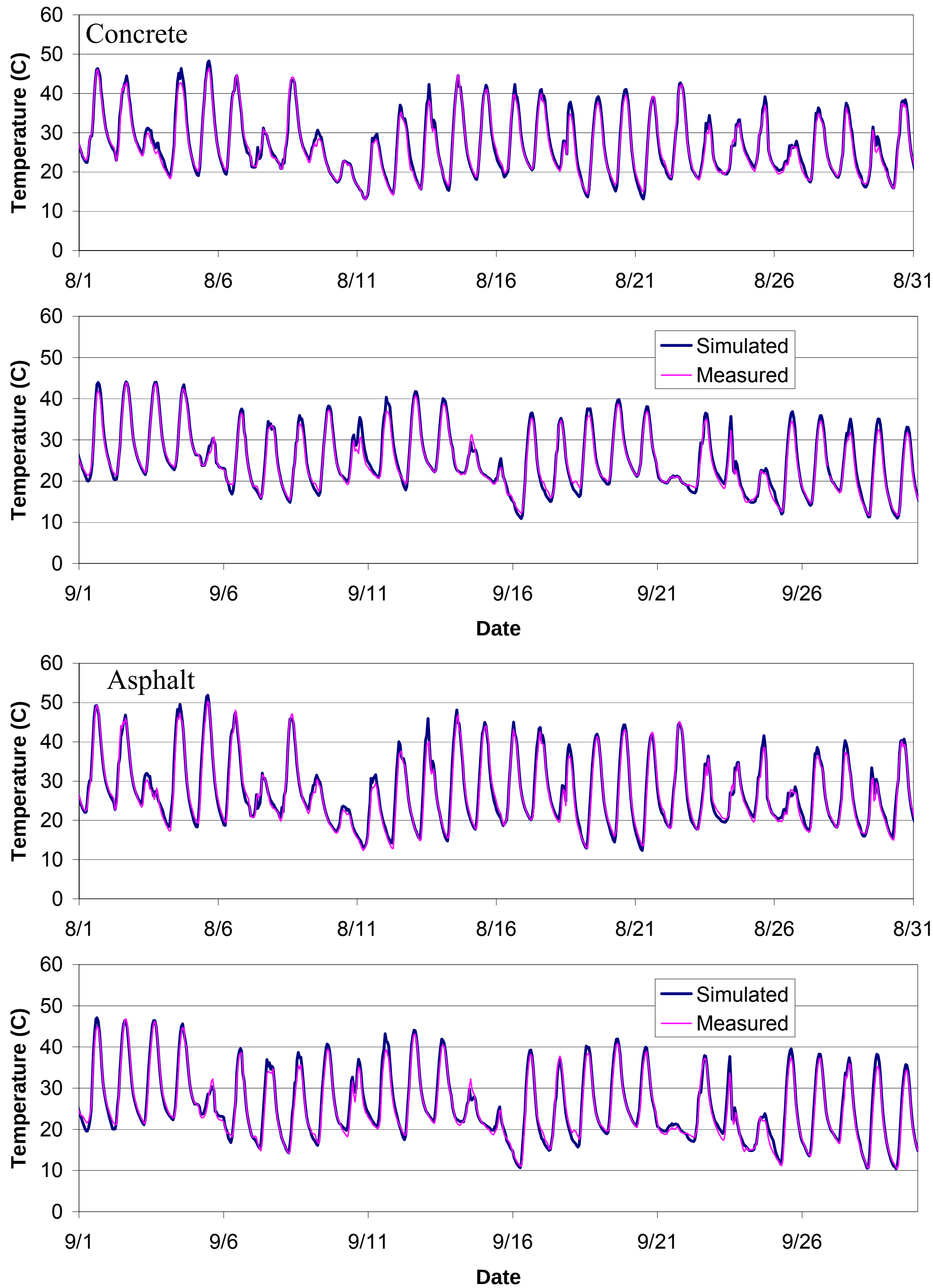

Figure 3.3. Simulated and measured pavement temperature (2.5 cm depth) for August and September, 2004, MnROAD test sections 33 (asphalt) and 38 (concrete), 1 hour time step.

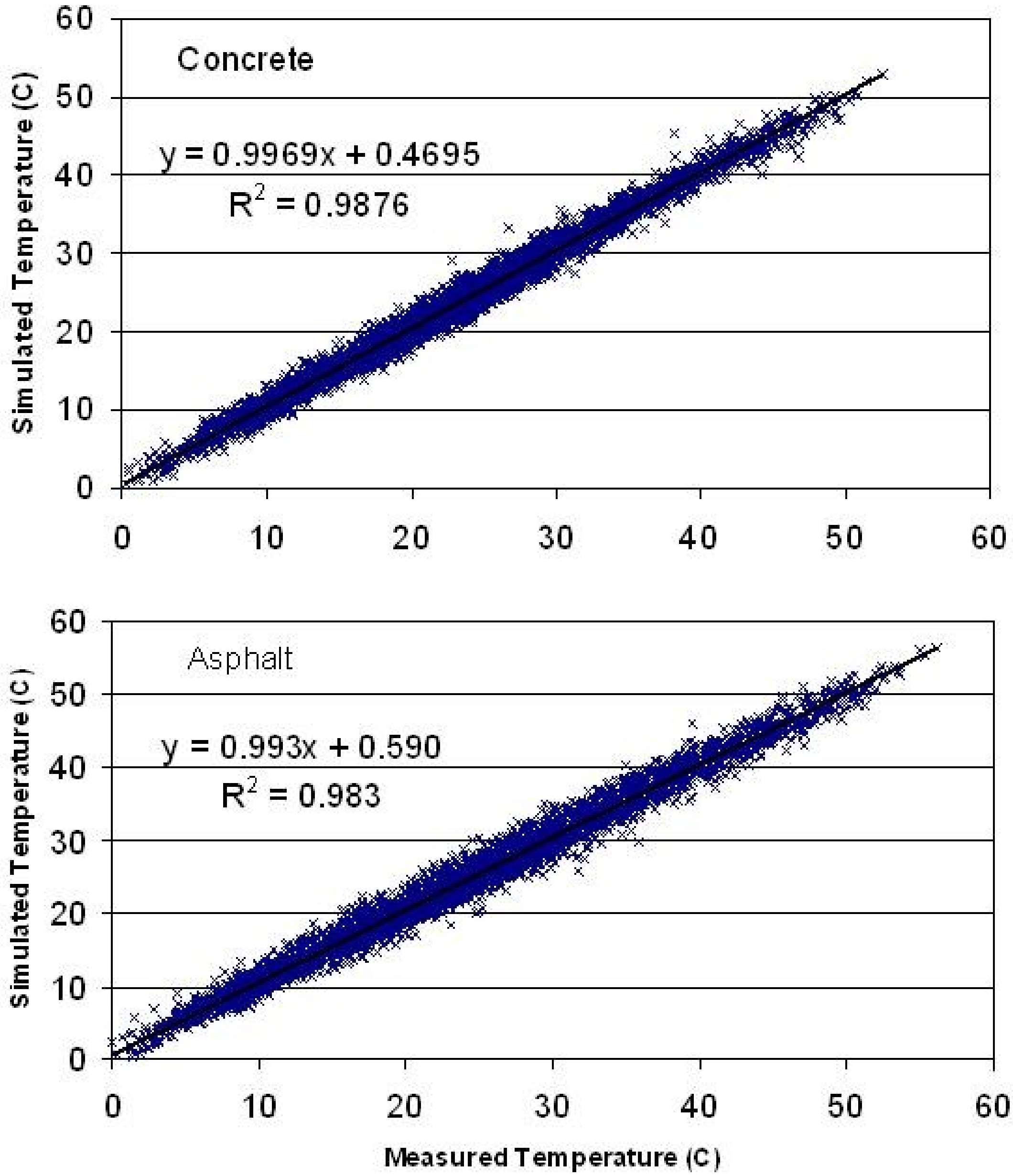

Figure 3.4. Hourly simulated versus measured pavement temperature (2.5 cm depth) for April - September, 2004, MnROAD Test cells 33 (asphalt) and 38 (concrete). The overall RMSE is 1.2 °C for concrete and 1.5 °C for asphalt.

Table 3.3. Summary of simulation accuracy for the MnROAD asphalt test section, for April – October, 2004, 1 hour time step. All RMSE values have units of °C.

	r^2 overall	RMSE overall	RMSE daily max	RMSE daily min	RMSE daily mean	RMSE daily ampl.
April	0.983	1.47	1.42	1.09	1.13	1.30
May	0.973	1.45	1.43	1.13	0.96	1.58
June	0.976	1.50	1.23	0.67	0.58	1.55
July	0.979	1.51	1.08	0.77	0.59	1.42
August	0.975	1.59	2.02	0.81	0.93	1.97
September	0.978	1.50	1.94	0.89	0.94	2.19
All	0.982	1.51	1.57	0.90	0.88	1.70

Table 3.4. Summary of simulation accuracy for the MnROAD concrete test section for April – October, 2004, 1 hour time step. All RMSE values have units of °C.

	r^2 overall	RMSE overall	RMSE daily max	RMSE daily min	RMSE daily mean	RMSE daily ampl.
April	0.975	1.43	1.14	0.91	0.99	1.22
May	0.980	1.13	1.23	0.91	0.76	1.15
June	0.988	0.96	1.02	0.85	0.51	1.39
July	0.987	1.05	1.29	1.14	0.67	1.56
August	0.982	1.17	1.71	0.82	0.76	1.84
September	0.982	1.19	1.91	0.93	0.72	2.28
All	0.986	1.17	1.42	0.93	0.75	1.62

Table 3.5. Summary of simulation accuracy for the MnROAD asphalt test section for six years of simulations (2000-2005), April 1 to October 31, 15 minute time step. All RMSE values have units of °C.

	r^2 hourly	RMSE hourly	RMSE daily max	RMSE daily min
2000	0.982	1.60	1.85	1.31
2001	0.981	1.58	2.52	1.43
2002	0.970	1.85	2.28	1.57
2003	0.980	1.44	2.13	1.51
2004	0.981	1.38	2.07	1.32
2005	0.962	1.73	1.90	1.27

3.6 Full year simulations of pavement temperature

Winter conditions can be particularly damaging to pavement because 1) pavement, particularly asphalt, has lower elasticity and becomes more brittle at lower temperature and 2) low temperatures cause the pavement to shrink, producing tensile stress and cracking. Numerical simulation of pavement temperature for the winter is more difficult than for other seasons because surface properties change as snow and ice layers form on the pavement surface. Snow layers reduce surface heat transfer by increasing albedo and decreasing emissivity, and freeze/thaw cycles in the presence of moisture complicate heat conduction through the subgrade and soil layers. For the purposes of this project, wintertime pavement temperature simulations were performed with the previously described model, but allowing seasonal variation of surface parameters (albedo, emissivity). A snow/ice layer was not added to the model, since snow/ice cover is usually not persistent on traveled roads, and the depth and the period of snow/ice cover are not easy to predict with reliability because of localized variations of snowfall intensity, wind drift, plowing schedules and traffic densities.

Simulations of Test cell 33 temperatures for the entire year of 2004 with fixed parameters shows significant variation in simulation errors with season (Figure 3.5, upper panel). The introduction of a seasonally varying albedo significantly improved the simulated pavement temperatures, such that the RMSE was under 1.8°C for the entire year (Figure 3.5, lower panel). The calibrated, seasonally varying albedo is given in Figure 3.6. The seasonal variation is attributed to the variations in sun angle and pavement surface properties from moisture. Allowing seasonal variation of emissivity did not significantly improve the simulation results, so that all results presented used a fixed value of 0.94.

A fresh snow cover insulates any surface including pavements and reflects much more short wave (solar) radiation than most bare surfaces (Henneman and Stefan,1999). During periods of snow cover at MnROAD, simulated pavement temperatures temporarily diverge from actual temperatures, but recover quickly when the snow cover is removed (Figure 3.7, upper panel). A snow/ice cover introduces smaller errors to the simulated temperatures at greater depth below the pavement surface, but the errors may persist for several weeks (Figure 3.8, lower panel).

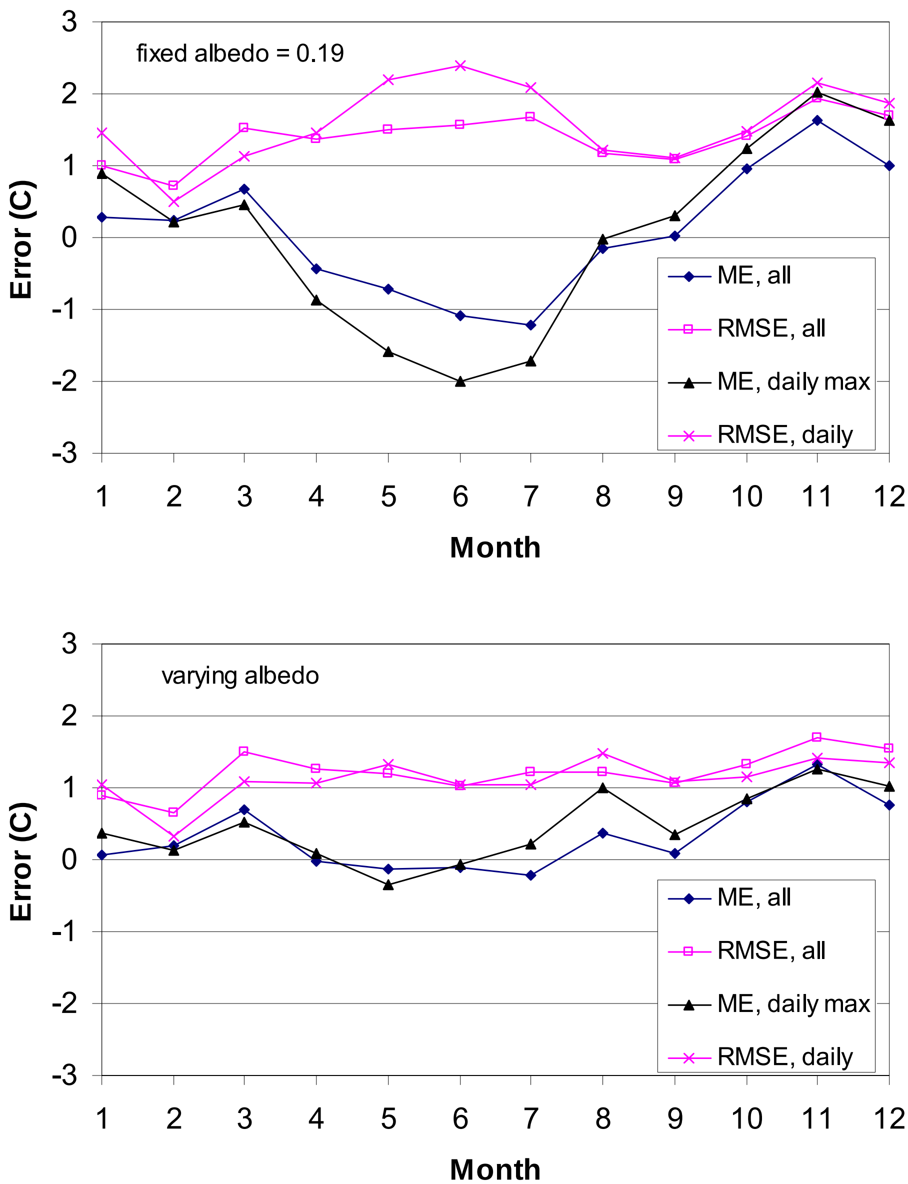

Figure 3.5. Error in pavement temperature (2.5 cm depth) simulation by month for MnROAD test cell 33, 2004 for fixed surface albedo=0.19 and for varying albedo (Figure 3.6). RMSE is root-mean-square error, ME is mean error.

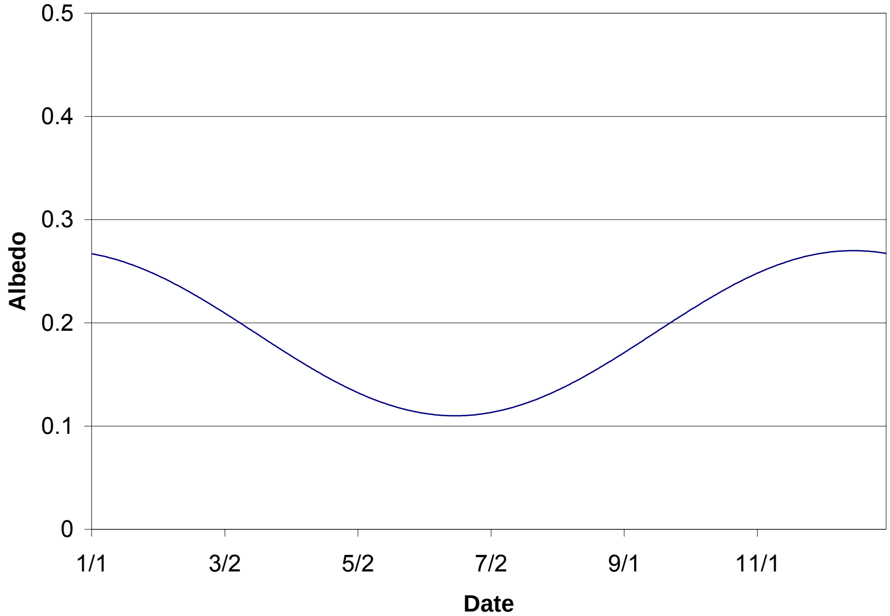

Figure 3.6. Calibrated seasonal variation of surface albedo for Test cell 33, 2004. albedo = 0.19+0.08*Cos(2π (cd+15)/365), where cd is the calendar day.

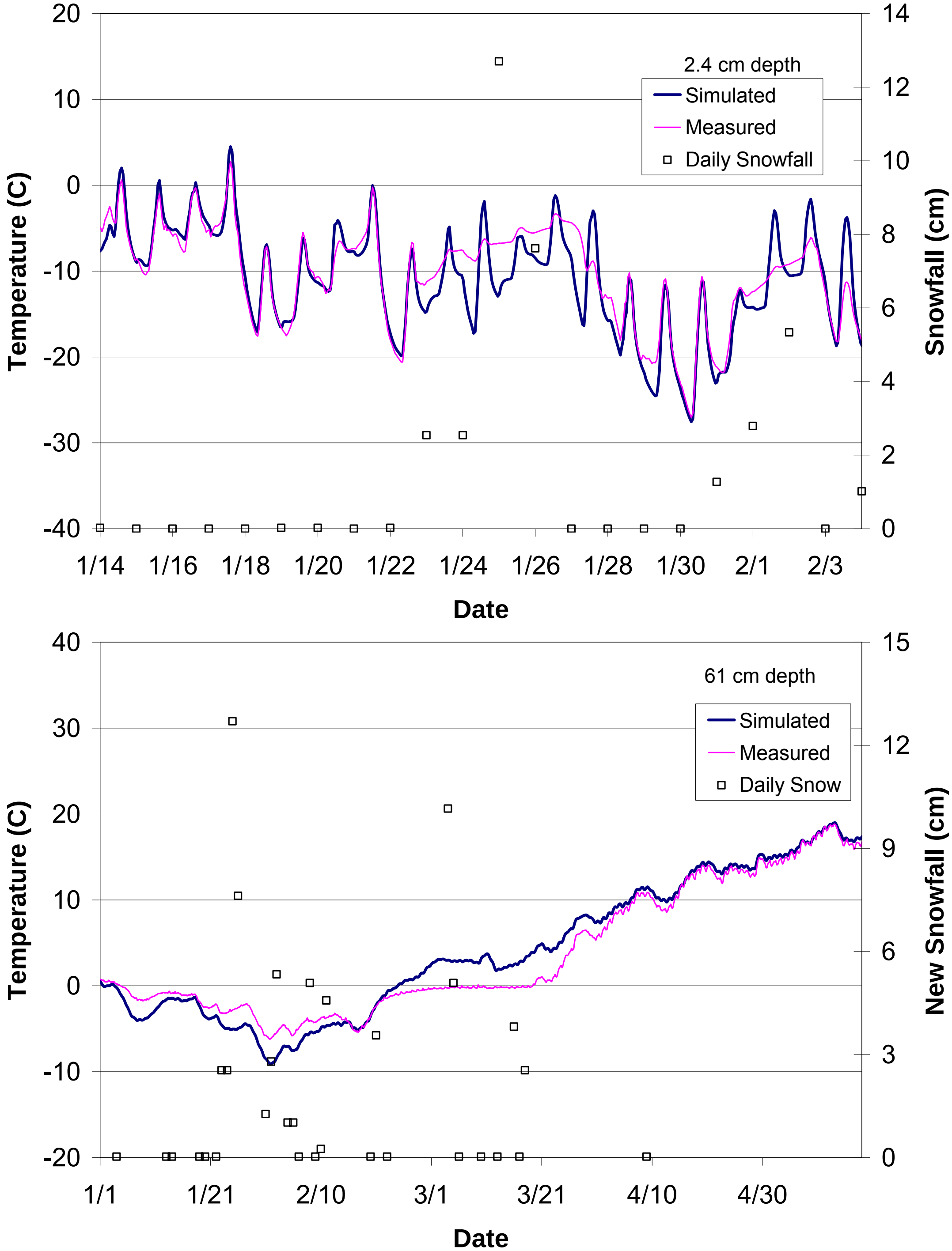

Figure 3.7. Simulated and measured temperature vs. time for 2.5 cm depth (upper panel) and 60 cm depth (lower panel). Daily new snow fall is measured at the Maple Lake airport.

3.7 Pavement temperature simulation for a RWIS

The MNDOT roadside weather information stations (RWIS) provide an additional opportunity to evaluate the pavement temperature model. The RWIS station chosen for this study is located on Highway 10 at mile marker 161.3, near St. Cloud (RWIS station Benton 64). This station is relatively well instrumented, including air temperature, humidity, wind speed and direction, rainfall, solar radiation, pavement surface temperature, and subsurface temperature. All data are recorded at 10 minute intervals. Data for 2004 were downloaded from the MnDOT/UMD RWIS web site

www.d.umn.edu/~tkwon/RWISarchive/RWISarchive.html

Converting the RWIS data to a long term series, e.g. 1 month, is a relatively slow process, because the data are extracted from the archive as a separate text file for each parameter and for each day. A two week (July 1 to July 15, 2004) time series of the climate parameters and pavement temperatures was assembled for this study). The solar radiation and wind speed values obtained from the RWIS station were clearly erroneous. Solar radiation values reported in units of J/m^2 for each 10 minute time period were therefore corrected to actual units of kJ/m^2, based on comparisons of the RWIS data to solar radiation data from the MnROAD site for the same time period. Wind speed values reported in units of m/s were corrected to actual units of tenths of m/s, based on information on the raw data format. Subsurface temperatures are also measured at the RWIS site, but the actual depth of the two temperature sensors could not be found. Information on the web site of the sensor manufacturer (SSI) suggests that the upper sensor is typically buried at a depth of 17 inches (43 cm).

A simulation of pavement temperature for the RWIS site was performed using the 2 weeks of climate data from the RWIS station (July 1 to July 15, 2004). Pavement and soil temperatures for the MnROAD Test cell 33 for July 1, 2004 were used as an initial condition for the simulation. All model parameters were kept at the same value as those used for Test cell 33 (Table 3.1). The simulated pavement and soil temperatures are compared to the temperatures obtained from the RWIS station in Figures 3.8 and 3.9. The simulated mid-day surface temperature exceeds the measured surface temperature by up to 5 °C, and the overall RMSE is 2.4 °C. The measured surface temperature agrees more closely with the simulated pavement temperature at 1 cm depth (RMSE=2.0 °C), as shown in the lower panel of Figure 3.8. This modest discrepancy in surface temperature may be due to inaccuracies in the climate data, or the model parameters, or the temperature sensing method used at the RWIS station. The measured sub-surface temperature is in reasonable agreement with the simulated temperature at 43 cm (Figure 3.9).

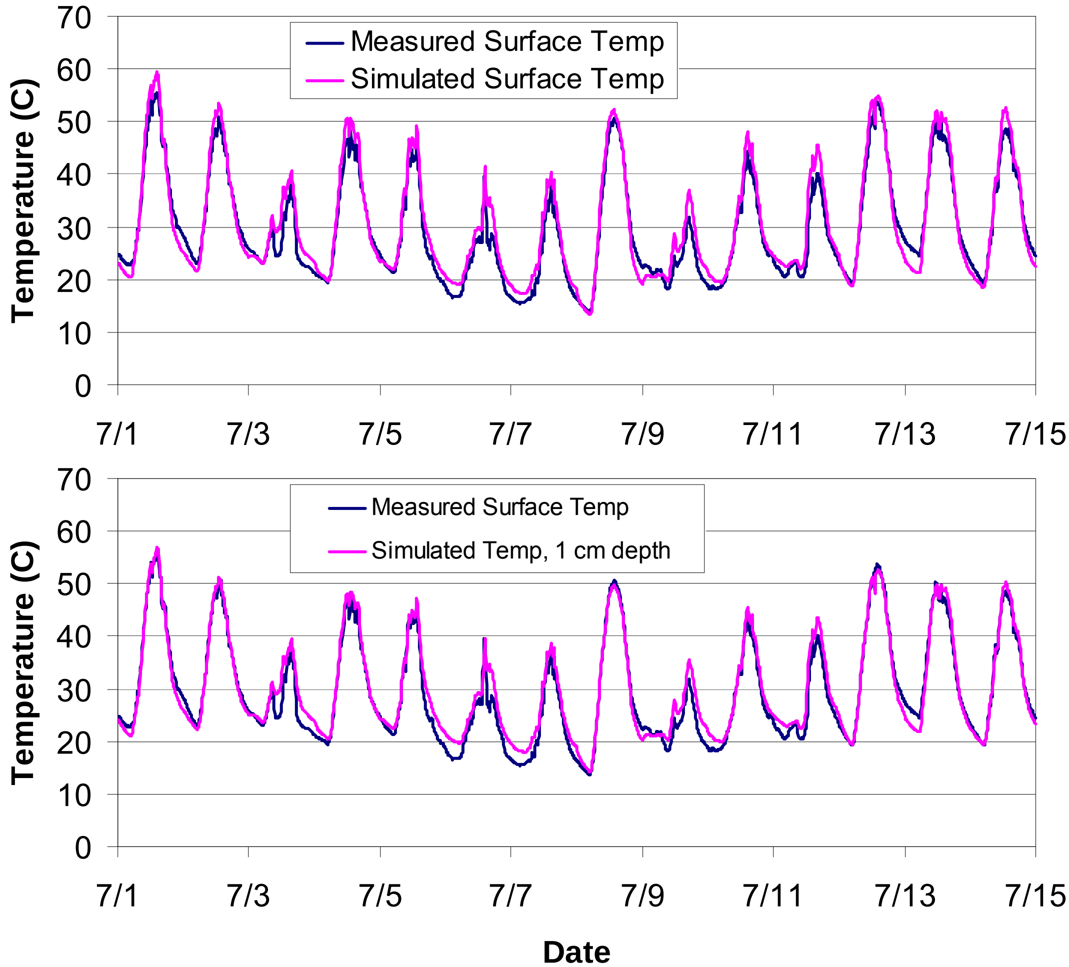

Figure 3.8. Measured and simulated pavement temperature for Highway 10 at mile marker 161.3, near St. Cloud (RWIS station Benton 64) for July 1 to July 15, 2004.

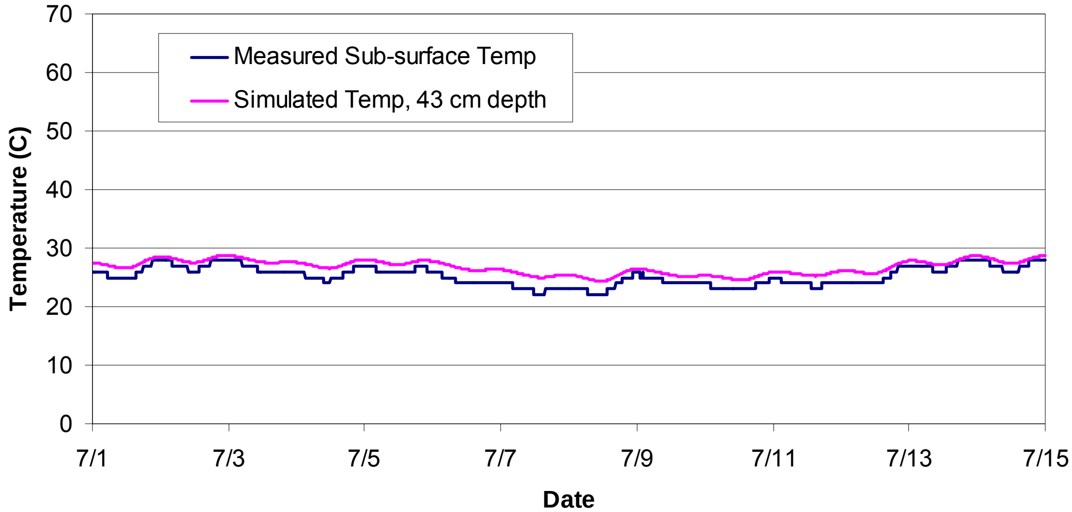

Figure 3.9. Measured and simulated subsurface (43cm=17in) temperature for Highway 10 at mile marker 161.3, near St. Cloud (RWIS station Benton 64) for July 1 to July 15, 2004.

3.7 Conclusions from pavement temperature simulations

Overall, the pavement temperature model developed at SAFL is able to simulate asphalt temperature to within 1 to 2°C RMSE. Pavement temperature simulation is more difficult for winter conditions, due to intermittent snow/ice cover and freeze-thaw processes. The pavement temperature model seems suitable to model pavement and subgrade temperatures at RWIS sites. It can therefore provide a tool to check the consistency of the pavement temperature data measured at RWIS sites around the State of Minnesota and at the MnROAD site, by predicting expected pavement temperature time series from the measured climate data at the RWIS sites with the model calibrated against the much more detailed data from the MnROAD site. Substantial differences between predicted and measured pavement temperatures at an individual RWIS would be indicative of a need for quality control of the instrumentation, while widespread substantial differences could indicate regional differences in pavement responses to weather.

The pavement temperature simulations are useful to identify the processes and weather conditions that produce the extreme changes in pavement temperature parameters that lead to pavement degradation, for example, rapid decreases in surface temperature due to the evaporation of precipitation from warm pavement.

The pavement temperature model is most sensitive to surface parameters, including the surface albedo (reflectivity) and emissivity. However, the magnitude of sensitivity is not large, e.g. 0.5 °C change in temperature for a 10% change in emissivity. It would be difficult to accurately extract pavement surface properties from measured temperature data alone, and the pavement parameters extracted in the model calibration process have significant uncertainty. On the other hand, these low sensitivities suggest that a calibrated model should give robust results for locations, other than MnROAD, e.g RWIS sites, if suitable climate data are available.

4. RECOMMENDATIONS

1) It is recommended that the pavement temperature characteristics identified and analyzed in Section 2 of this report be linked to the known chemistry and mechanics of asphalt pavement deterioration processes such as volatilization of compounds, crack formation due to contraction, fatigue of the pavement etc. If this gap can be filled, meaningful temperature characteristics can be obtained from pavement data or simulations.

2) Nine of the RWIS stations in Minnesota are equipped with solar radiation sensors, and thus provide all necessary climate data to simulate pavement temperature. Simulated pavement temperature should be in reasonable agreement with the pavement surface temperature reported by the RWIS stations, with no additional model calibration. This type of quality check is recommended. Also recommended are additional investigations on the incorporation of freeze-thaw cycles into the pavement temperature model.

3) Also recommended are additional investigations on the incorporation of freeze-thaw cycles into the pavement temperature model.

Acknowledgements
Funding for this project was provided by a …., through Thomas Wodd, MnDOT Office of Materials
The authors would like to acknowledge the following peoplMNDOT staff
Climate and pavement temperature data from the MnROAD site were provided by Ben Worel and Tim Clyne, MnDOT Office of Materials.
RWIS data was obtained from the Mn/DOT Statewide R/WIS Archive Download Page, http://www.d.umn.edu/~tkwon/RWISarchive/RWISarchive.html

References

Edinger, J.E., D.K. Brady and J.C. Geyer (1974). “Heat Exchange and Transport in the Environment”. The Johns Hopkins Univ., Dept. of Geogr. and Env. Eng., Report 14 Cooling Water Studies for the Electric Power Research Institute, RP-49, Palo Alto, CA.

Henneman, H. and H.G. Stefan (1999). “Albedo models for snow and ice on a freshwater lake”. Cold Regions Science and Technology 29:31-48.

Appendix I: Surface heat transfer formulation

The net vertical heat transfer at the soil or pavement surface includes components due to long wave radiation, short wave (solar) radiation, evaporation, and convection. The heat transfer formulations used in this study are based on those given by Edinger (1974) for lake and reservoir surfaces, but are applied to pavement and soil by adjusting parameters appropriately. Equations A.1 through A.9 give the formulations used to calculate the net surface hat flux, h_{net}.

(A.1) $h_{net} = h_{rad} - h_{evap} - h_{conv} - h_{ro}$

(A.2) $h_{evap} = \rho_a L_v \left(C_{fc}\, u_s + C_{nc} \Delta\theta_v^{\,0.33} \right) \left(q_{sat} - q_a \right)$

(A.3) $h_{conv} = \rho_a c_p \left(C_{fc}\, u_s + C_{nc} \Delta\theta_v^{\,0.33} \right) \left(T_s - T_a \right)$

(A.4) $h_{rad} = h_s + h_{li} - h_{lo}$

(A.5) $h_s = (1 - \alpha) R_s$

(A.6) $h_{li} = \varepsilon\sigma \left(CR + 0.67 \cdot (1 - CR) e_a^{\,0.08} \right) T_{ak}^4$

(A.7) $h_{lo} = \varepsilon\sigma T_{sk}^4$

(A.8) $u_s = CS_h\, u_{10}$

(A.9) $h_{ro} = \dfrac{P}{\Delta t} (\rho cp)_w \left(T_s - T_{dp} \right) \left(\dfrac{\beta}{1+\beta} \right) \; ; \; \beta = \dfrac{\delta \left(\rho c_p \right)_{pave}}{2P \left(\rho c_p \right)_{water}}$

Table A.1. Surface heat transfer parameter definitions.

C_{fc}	forced convection transfer coefficient	T_{dp}	dew point temperature, °C
C_{nc}	free convection transfer coefficient	T_{ak}	air temperature, °K
CR	cloud cover ratio (0 – 1)	T_s	surface temperature, °C
CS_h	wind sheltering coefficient	T_{sk}	surface temperature, °K
c_p	specific heat	u_s	adjusted wind velocity
h_{rad}	net incoming surface radiation	u_{10}	wind velocity at 10 m above the surface
h_s	short wave radiation absorbed at surface	α	surface albedo
h_{li}	incoming long wave radiation	$\Delta\theta$	difference in virtual temperature
h_{lo}	outgoing long wave radiation	$_v$	between ground and air
h_{ro}	runoff heat transfer	δ	conduction layer thickness
L_v	latent heat of vaporization	ε	surface emissivity
P	precipitation depth	ρ	density
R_s	incoming solar radiation	σ	Stefan-Botzmann constant
T_a	air temperature, °C		

Many of the surface heat transfer terms are non-linear, i.e. the heat flux depends on the surface temperature, and the outgoing long wave radiation is strongly dependent on surface temperature. A simple linearization was used to help keep numerical stability at longer time steps. The outgoing long wave radiation is linearized as follows:

(A.10) $h_{lo} = \varepsilon\sigma T_{sk}^4 + 4\varepsilon\sigma T_{sk}^3 \left(T'_{sk} - T_{sk}\right)$

where T'_{sk} and T_{sk} are the value of the surface temperature for the current and previous time steps.

The heat transfer from the pavement surface to surface runoff (h_{ro}) is estimated as follows. The model assumes that the surface runoff, assumed to be initially at dew point temperature, and pavement surface must equilibrate to the same temperature over the time step (Δt), as shown in Figure A.1. To achieve this equilibrium, a convective heat flux Q_{ro} can be calculated, which draws heat out of a thin layer of pavement at the surface with thickness δ. The size of δ can be estimated from the thermal properties of the pavement and the time step, based on analytic solutions for heat conduction into an infinite slab subject to a change in surface temperature (Eckert and Drake, 1972).

(A.11) $\delta = \sqrt{4\alpha\Delta t}$

where α is the thermal diffusivity and Δt is the time step. For a time step of 15 minutes and a thermal diffusivity of 4×10^{-6} m^2/s, $\delta = 3.8$ cm. An equation for the heat balance for the water film layer and the pavement may then be written as:

(A.12) $Q_{ro} = h\left(\rho c_p\right)_w \left(T_s - T_{ro}\right) = -\frac{\delta}{2}\left(\rho c_p\right)_p \left(T_s - T_{so}\right)$ (J/m^2)

where $(\rho c_p)_p$ and $(\rho c_p)_w$ are (density · specific heat) for the pavement and water, and the factor (δ/2) takes into account that the temperature change in the pavement decreases with depth, whereas the temperature change in the water film as assumed to be uniform across the thickness h. If the dew point temperature and the initial surface temperature are know, so Equation A.12 can be solved for T_s and Q_{ro}.

(A.13) $T_s = \frac{1 + \beta T_{so}}{1 + \beta}$, where $\beta = \frac{\delta\left(\rho c_p\right)_p}{2h\left(\rho c_p\right)_w}$

(A.14) $Q_{ro} = h\left(\rho cp\right)_w \left(T_{so} - T_{dp}\right)\left(\frac{\beta}{1 + \beta}\right)$ (J/m^2)

Using Equation A.14, the heat flux from the pavement to the runoff may be estimated for each time step based on the total precipitation in each time step, and is simply added to the atmospheric heat flux components. At any given time, the actual runoff depth is typically much less than the total precipitation depth, but the entire precipitation depth can still be expected to equilibrate with the pavement surface, so that applying the entire precipitation depth over the time step is equivalent to applying the same amount as a series of thin layers over shorter time steps. For the one-dimensional model, there is no consideration of lateral variations in runoff temperature from upstream to downstream points.

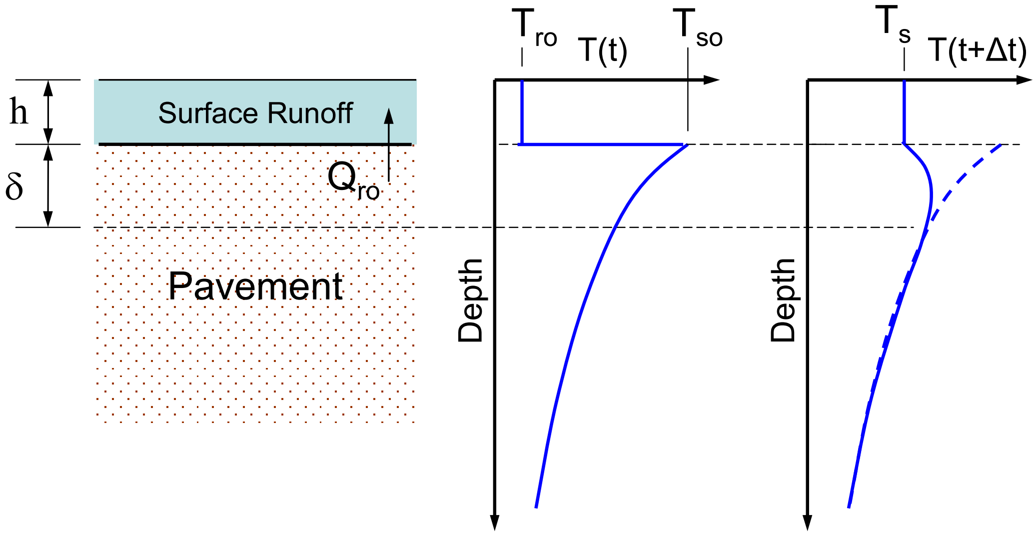

Figure A.1. Schematic of the formulation for heat transfer between surface runoff and the underlying pavement. Example temperature profiles show the temperatures in the pavement prior to a rainfall event (T(t)) and after a rainfall event (T(t+Δt), where the initial surface temperature (T_{so}) has equilibrated with the initial runoff temperature (T_{ro}) to yield the new surface and runoff temperature (T_s).